International Journal of Multiphase Flow, Volume 96, 2017, Pages 70-85
DOI:10.1016/j.ijmultiphaseflow.2017.07.005

Water-lubricated transport of high-viscosity oil in horizontal pipes: the water holdup and pressure gradient

Jing Shi, Liyun Lao, Hoi Yeung

Oil and Gas Engineering Centre, School of Water, Environment and Energy, Cranfield University, Cranfield MK43 0AL, UK

Abstract

This paper has investigated the water holdup and the pressure gradient of water-lubricated transport of high-viscosity oil flow in horizontal pipes. Experimental results on the water holdup and the pressure gradient of water-lubricated high-viscosity oil two-phase flow in a horizontal 1 inch pipe were discussed. Models for the prediction of the water holdup and/or the pressure gradient of core flow or water-lubricated flow were reviewed and evaluated. It was found that the water holdup of the water-lubricated flow is not only closely related to the input water volume fraction but also the degree of the oil phase eccentricity which is attributed to the oil phase Froude number. This can explain the inconsistency of the experimental results with regard to the relationship between the water holdup and the input water volume fraction in the literature. The applicability of the existing empirical or mechanistic models of water-lubricated high-viscosity oil flow were discussed and demonstrated. A modified correlation to the water holdup correlation of Arney et al. (1993) which was shown to be exclusively applicable for concentric core flow was introduced for stable water-lubricated flow, including both concentric and eccentric core flows. This correlation was evaluated and a fair applicability was shown. The accuracy of different models for the prediction of the pressure gradient of water-lubricated transport of high-viscosity oil was demonstrated to be not high in general. This is closely associated with the difficulty in accurately accounting for the influence of oil fouling on the pressure gradient.

Keywords: water-lubricated flow; high-viscosity oil-water; water holdup; pressure gradient, oil fouling.

Correspondence concerning this article should be addressed to J. Shi at jingshi1988@gmail.com

1 Introduction

At ambient temperature, heavy crude oil does not flow easily due to high viscosity. Technologies to enhance the mobility of heavy crude oil are required in both heavy oil production and transportation. The traditional approach for high-viscosity oil transport is to reduce the viscosity. This can be accomplished by heating, diluent addition or a combination of both. Water-lubricated flow technology provides an alternative to oil viscosity reduction technologies. In this method, high-viscosity oil is transported inside continuous water which lubricates the pipe. The most ideal flow regime is core annular flow (CAF) in which heavy oil is transported with a small amount of water. A number of studies have shown that the pipe normally fouls under flow conditions and operation procedures of practical importance (e.g., Arney et al., 1996; Joseph et al., 1999; Bannwart, 2001; McKibben et al., 2000a and 2000b; Sridhar et al., 2011; Al-Awadi, 2011; Alagbe, 2013; Shi and Yeung, 2017). Nevertheless, even with the existence of oil fouling film on the pipe wall, the pressure loss of the viscous oil flow with water-lubricating is still much lower than that without water-lubricating. Some pilot experiments showed that the water-lubricated flow with oil fouling can be operated for a long time without accumulation of oil on the pipe wall if properly controlled (Joseph et al., 1999; McKibben et al., 2000b).

Experimental investigation of the flow behaviours of water-lubricated flow is an essential approach to improve our knowledge on this particular two-phase flow. Most of the experimental studies on water-lubricated flow in the literature report results on flow patterns and pressure gradients. Another important parameter is the phase holdup as there may be slip between the phases. However, high-viscosity oil-water flow involves a very viscous fluid, which makes the measurement of phase holdup challenging. Experimental data on the phase holdup of water-lubricated high-viscosity oil two-phase flow in the literature is quite limited. Also, the available limited data sometimes suggest seemingly inconsistent flow characteristics of horizontal CAF. Both Oliemans et al. (1987) and Arney et al. (1993) reported that the water holdup of horizontal CAF is in general higher than the input water volume fraction, indicating an average oil-water slip ratio higher than 1. However, an average oil-water slip ratio of 1 for CAF in horizontal pipe was reported in Bannwart (1998). It is of importance to conduct experimental measurement of

the water holdup of water-lubricated flow to clarify the inconsistency and improve our understanding in flow characteristics.

Accurate prediction of the water holdup and pressure gradient of water-lubricated pipeline flow is desirable as it can provide guidance to the design and operation of engineering practice. Simple phenomenological/empirical and mechanistic/semi-empirical models take little account of the details across the flow direction, but they can be quite successful for predicting design parameters such as the pressure gradient and water holdup. Compared to three-dimensional numerical modelling, they are computationally cheap and can provide useful solutions for industrial applications. The phenomenological models treat the oil-water flow as one mixture fluid and comprise empirical correlations for the friction factor and the mixture fluid properties. The mechanistic models (i.e., two-fluid models) treat the immiscible fluids separately with their own sets of governing equations. The mechanistic models normally require closure relationships developed from experimental data to get solutions thus the mechanistic models are actually semi-empirical. Arney et al. (1993) and Brauner (1998) proposed models for ideal core annular flow. The flow is simplified as axis-symmetric and the influence of oil fouling on the pipe internal wall is not accounted for. It is expected that the above models would under predict the pressure gradients of water-lubricated flow in industrial applications. Evaluation of the models with data collected from experiments which are conducted in flow conditions of practical importance has not been reported. Therefore, the quantitative accuracy of these models for industrial applications of water-lubricated flow is not clear. Some empirical models proposed from experimental data conducted in flow conditions relatively closer to practical operations has also become available in the literature, such as Bannwart (2001), McKibben et al. (2000b) and McKibben et al. (2013). However, these models lack validation with independent experimental data. Three-dimensional numerical modelling can also be helpful for understanding some nature of water-lubricated flow. A number of numerical studies have been conducted to provide insight into the characteristics such as the shapes of interface waves and the stability of the core flow (e.g., Ooms et al., 1984; Bai et al., 1996; Ko et al., 2002; Li and Renardy, 2000; Ooms et al., 2013; Beerens et al., 2014; and Lee and Kang, 2016). However it is not yet a practical method to provide engineering solutions due to its high computational cost.

This study aims to conduct an experimental investigation of water lubricated transport of high-viscosity oil in horizontal pipes with focus on the water holdup and the pressure gradient of water-lubricated flow. Furthermore, the existing empirical and mechanistic models for the prediction of water holdup and/or pressure gradient will be evaluated with the experimental data to shed some light on the applicability of different models. The paper is structured as follows. A literature review on the measurement of water holdup of water-lubricated flow and the existing models of water-lubricated flow is first presented in Section 2. The experimental setup is described in Section 3. The experimental results and the evaluation of models with the experimental data are presented in Section 4. Conclusions are summarised in Section 5.

2 Literature review

2.1 Measurement of water holdup of water-lubricated flow

When two fluids flow simultaneously in a pipeline, the in situ volume ratio can be different from the input volume ratio. Differences in density and/or viscosity give rise to an important feature of two-phase flow - the occurrence of the ‘slip’ of one phase past the other, or the ‘hold-up’ of one phase relative to the other (one phase accumulating in the pipe) (Oliemans and Ooms, 1986).

A basic method to achieve phase holdup measurement is the sampling method. The theory of this method is straightforward - to get samples which can represent the in situ phase contents and obtain phase holdups after phase separation. Usually two quick-closing valves are used to trap fluids, and then the trapped fluids are measured with volume measurement instrumentation. Though the principle of this method is simple, the applicability of this method is fairly limited due to its essence of offline measurement. Also, for high-viscosity oil-water flow, it would be time consuming due to slow phase separation. Charles et al. (1961) applied this method in their pioneering work on oil-water two-phase flow with relatively low viscosity oils (6.29, 16.8 and 65 cP). After fluids were trapped with two quick-closing valves, a pig was used to drain liquids out to get the samples. Applying the sampling method, Arney et al. (1993) and Sridhar et al. (2011) reported studies which measured water holdups of oil-water flow for viscous oils by using a removable section with a pair of ball valves to trap fluids.

Photographs taken during experimental runs can also be made use of to extract information of water holdups of core annular flow. The water holdup information is determined upon the assumption that the shape of the oil core is perfectly circular with this method. Oliemans et al. (1987) applied this method to obtain the water holdup information. It is noted that the assumption of perfect circular oil core would lose its validity when the cross-section of the oil core is ellipse-like. Shi (2015) performed CFD simulation of CAF and the results demonstrated that the cross-section of the oil core is roughly circular for concentric core flow and more ellipse-like as the eccentricity of the oil core becomes high. Bannwart (1998) extracted wave speed from high-speed images of core flow by measuring the distance traveled by a wave crest between two marks and the corresponding elapsed time. The oil-water slip ratio was obtained via deducted relations between the slip ratio and the wave speed.

Intrusive methods such as conductivity probes and wire mesh are less likely to be feasible for water-lubricated high-viscosity oil-water flow due to oil adhesion. A non-intrusive method based on a capacitance probe was investigated by Strazza et al. (2011a). A capacitance probe with two concave electrodes was developed specifically for core annular flow. Oil holdup was obtained assuming a perfect circular oil core. As mentioned above, this assumption would not be appropriate for eccentric core flow, which is one possible source of systematic errors. A good agreement between measurements from the developed capacitance probe and the quick-closing valves was demonstrated in the above authors' experimental tests, with uncertainties within ±5% for most of the tests. This approach shows some promise on the use of capacitance probes for the measurement of phase holdups of fluids with conductive continuous phase. The radiation methods such as Gamma densitometers and X-ray are expensive and they require costly health and safety protection measures. Also, for highly viscous oil, the oil density is normally higher than traditional crude light oil and is close to the water density. The small density difference between heavy oil and water leads to similar attenuation coefficients, which makes the radiative methods less attractive for the measurement of high-viscosity oil-water flow.

A summary of experimental studies on high-viscosity oil-water flow in horizontal pipes in the literature is listed in Table 1. The measurement of water holdup (H_w) was only conducted in a few studies among which the sampling approach was applied predominantly. The overall

advantage of the sampling approach with regards to measurement accuracy, feasibility and construction expense make it a preferable method to measure the phase holdup for high-viscosity oil-water flow.

2.2 Empirical and mechanistic models of water-lubricated flow

Arney et al. (1993)

Arney et al. (1993) deduced a counterpart ($\Re$) similar to the Reynolds number by applying the Navier-Stokes equation to the perfect liquid-liquid laminar core annular flow. The deduced Reynolds number, $\Re$, is defined as

$$\Re = \frac{\rho_m U_m D}{\mu_w}[1 + \eta^4(\mathrm{m} - 1)] \tag{1}$$

$$\eta = \frac{D_o}{D} = \sqrt{1 - H_w} \tag{2}$$

$$m = \frac{\mu_w}{\mu_o} \tag{3}$$

Where $\rho_\mathrm{m} = (1 - H_w)\rho_\mathrm{o} + H_w\rho_\mathrm{w}$, ρ_m, ρ_o and $\rho_w$denote the mixture density, oil density and water density, respectively; U_m the mixture velocity, $U_\mathrm{m} = U_\mathrm{so} + U_{sw}$, U_so and U_{sw} denote the superficial oil velocity and water velocity, respectively; D_o the oil core diameter; D the pipe internal diameter;

μ_w the water viscosity; μ_o the oil viscosity; H_w the water holdup. A reliable estimate of D_o (or H_w) is needed for the calculation of $\Re$, hence the pressure gradient. An empirical correlation between water holdup, H_w, and input water volume fraction, C_w, was given as

$$H_w = C_w[1 + 0.35(1 - C_w)] \tag{4}$$

The friction factor for the perfect laminar CAF, λ, is expressed as

$$\lambda = \frac{64}{\Re} \tag{5}$$

For turbulent flow, the Blasius formula was adopted, thus

$$\lambda = \frac{0.316}{\Re^{0.25}} \tag{6}$$

Knowing the friction factors, the pressure gradient ($-\frac{dp}{dz}$) of core annular flow can be estimated following the Darcy-Weisbach equation:

$$-\frac{dp}{dz}=\frac{\lambda}{D}\frac{\rho_m U_m^2}{2} \tag{7}$$

As the $\Re$ in the model of Arney et al. (1993) is deduced theoretically for perfect laminar CAF and oil fouling on the pipe inner wall is not considered in the model, it is anticipated that this model would under predict the pressure gradient of high-viscosity oil CAF in which oil fouling exists.

Brauner (1998)

Brauner (1998) applied the two-fluid approach to model concentric core annular flow. The integral forms of the momentum equations for the annulus (a) and the core (c) are:

$$-A_a\left(\frac{dp}{dz}\right)-\tau_a S_a+\tau_i S_i+\rho_a A_a g sin\beta=0 \tag{8}$$

$$-A_c\left(\frac{dp}{dz}\right)-\tau_i S_i+\rho_c A_c g sin\beta=0 \tag{9}$$

where A denotes the cross-section area, τ the shear stress, S the area of the contact interface, ρ the phase density, g the gravitational acceleration, and β the pipe inclination angle; the subscriptions a, c, and i denote the annular phase, the core phase, and the interface, respectively.

The two-fluid model can be numerically solved. Also, for the case of horizontal laminar core with either laminar or turbulent annular phase, simple explicit solutions can be derived (refer to Brauner (1998) for detail).

The model of Brauner (1998) applied the two-fluid approach to concentric core annular flow. As mentioned by the author herself, the predicted pressure gradient via this model may underestimate measured values in CAF operation due to the increase of wall friction associated with oil fouling and eccentricity of the oil core.

Bannwart (2001)

Bannwart (2001) proposed to use the traditional expressions of the pressure gradient with a modified mixture viscosity and modified friction factor coefficients.

For laminar-laminar perfect core annular flow, the pressure gradient can be expressed as

$$-\frac{dp}{dz}=64\left(\frac{\rho_m U_m D}{\mu_m}\right)^{-1}\frac{\rho_m U_m^2}{2D}=\frac{32\mu_m U_m}{D^2} \tag{10}$$

)

where $\rho_{\mathrm{m}} = H_o\rho_{\mathrm{o}} + (1 - H_o)\rho_{\mathrm{w}}$; μ_m is the mixture viscosity, and it is defined as $\frac{1}{\mu_m} = \frac{{H_o}^2}{\mu_o} + \frac{1-{H_o}^2}{\mu_w} \cong \frac{1-{H_o}^2}{\mu_w}$; H_o is the oil holdup, $H_o = \frac{1}{1+s\frac{U_{sw}}{U_{so}}}$ with s denoting the slip ratio of the two fluids. It is noted that this parameter is usually unknown as well. Bannwart (2001) reported different values of s for different flow systems based on wave speed measurement; s=1 was adopted for simplicity when it is unknown.

For laminar-turbulent core annular flow (when the annulus Reynolds number $\mathrm{Re}_{sw} = \frac{\rho_w U_w D}{\mu_w} > 2000$), the pressure gradient can be expressed as

$$-\frac{dp}{dz} = b\left(\frac{\rho_m U_m D}{\mu_m}\right)^{-n}\frac{\rho_m U_m^2}{2D} \tag{11}$$

where $\frac{1}{\mu_m} = \frac{H_o}{\mu_o} + \frac{1-H_o}{\mu_w} \cong \frac{1-H_o}{\mu_w}$, and b and n are coefficients; instead of the normally used coefficients of b and n in single phase flow, e.g., b =0.316 and n =0.25, the coefficients were determined from regression of experimental data in Bannwart (2001). According to the author, the coefficients account for the wall conditions such as oil fouling and wall roughness in the two-phase flow. Using this method to fit two groups of experiments of high-viscosity oil-water flow in steel and cement lined pipes respectively, the parameters obtained by the above author are b =0.305, n =0.159 for cement lined pipe and b =0.066, n =0.047 for oil fouled steel pipe with s=1.

The model of Bannwart (2001) requires three unknowns, namely the slip ratio of two fluids, s, and two friction factor coefficients, b and n, which are supposed to be determined from experiments. A slip ratio of 1 is recommended when it is unknown, while b and n are not specified. The general applicability of this model is limited.

McKibben et al. (2000b) and McKibben et al. (2013)

McKibben et al. (2000b) proposed a correlation from their experimental data to predict the pressure gradient of water-lubricated heavy oil flow. This model is also based on the traditional expression of the pressure gradient. A modified Fanning friction factor, f_m, was adopted to roughly account for the water lubrication effect empirically.

$$-\frac{dp}{dz} = \frac{2f_m}{D}\rho_w {U_m}^2 \tag{12}$$

$$f_m = \frac{1410}{\mathrm{Re_w}} \tag{13}$$

$$\mathrm{Re_w} = \frac{DU_m\rho_w}{\mu_w} \tag{14}$$

A new empirical correlation for the Fanning friction factor was proposed by McKibben et al. (2013) accounting for more parameters' influences. The new model follows

$$-\frac{dp}{dz} = \frac{2f_m}{D}\rho_m {U_m}^2 \tag{15}$$

$$f_m = 15{\mathrm{Fr}_m}^{-0.5} {f_w}^{1.3} {f_o}^{0.32} {C_w}^{-1.2} \tag{16}$$

$$\mathrm{Fr}_m = \frac{U_m}{\sqrt{gD}} \tag{17}$$

where Fr_m is a Froude number that accounts for the difficulty in establishing stable water-lubricated flows for heavy oils at low velocities, $\mathrm{Fr}_m > 0.35$; f_w is the Fanning friction factor for the aqueous phase; f_o is the Fanning friction factor for oil; and C_w is the total volume fraction of the aqueous phase.

Essentially, the empirical models proposed by McKibben et al. (2000b) and McKibben et al. (2013) are similar to that of Bannwart (2001). Both models adopted the traditional expressions of the pressure gradient for single phase flow with modifications/correlations of the friction factors and/or mixture properties. The model of Bannwart (2001) has coefficients which are not specified but to be determined from experimental data. The models given in McKibben et al. (2000b) and McKibben et al. (2013) have no unknown coefficients. The coefficients were determined from experimental data with a wide coverage of oils (viscous lube oil, heavy crude oil and bitumen, viscosity ranging from 620 to 91 600 cP) and nominal pipe diameters (50, 100 and 260 mm). Due to this fact, it is likely that the empirical models of McKibben et al. (2000b) and McKibben et al. (2013) can give some reasonable predictions for particular scales such as when flow conditions are within their experimental coverage. The models of Bannwart (2001) and McKibben et al. (2000b) and McKibben et al. (2013) have not been evaluated in the literature. These models need validation with independent experimental data sets.

A brief summary of the above models is presented in Table 2.

3 Experimental setup

3.1 General description

The experimental setup is shown in Figure 1. The oil was stored in a tank and its temperature was controlled by a chilling and heating system to get a desired oil viscosity. Lube oil Total CYL 680 was used (see Table 3 for the physical property of the oil) in the experiments. The oil was pumped by a progressive cavity pump (PCP) to the test rig. The oil flow was metered using a Coriolis flow meter (Endress+Hausser's Promass 83I DN 50) which output mass flow rate, density and viscosity with measurement accuracy of ±0.1% o.r. (of reading), ±0.5 kg/m^3 and ±0.5% o.r., respectively. The water was also stored in a tank and pumped by a PCP. The water flow was metered using an electromagnetic meter (Endress+Hauser's Promag 50P DN 50) with a range of 0~2.18 m^3/hr and accuracy of ±0.5% o.r. The oil flow and water flow meet at the T-junction then flow concurrently through a horizontal multiphase flow test line; a more detailed description of the multiphase flow test line is presented in the following section. Raw data acquired from online instrumentations, including the flowmeters, pressure transducers and temperature sensors were saved to a desktop computer using a National Instruments (NI) LabVIEW data acquisition system. After the multiphase flow test line, the fluids were collected into a gravity separator. A residence time of around 24 hours was given for complete separation of oil and water. On separation of the phases, oil was recycled and pumped back to the oil tank while water was disposed of properly. The oil density showed little change after separation thus the oil after separation is regarded as pure oil.

3.2 Multiphase flow test line

The multiphase flow test line is the main part of the test rig where the flow is developed and the flow information is collected. It was made up of transparent Perspex and clear PVC pipes. The internal diameter of the pipe, d, is 26 mm. The horizontal pipeline has a length of around 6.5 m. A detailed introduction of the multiphase flow test line is presented as follows.

The visual observation and pressure drop measurement section

Downstream the fluids mixing point, two gauge pressure transducers and one differential pressure transducer were installed to measure the pressure drop (see Figure 1). The two gauge pressure transducers were positioned at 2.04 m (78 d) and 3.77 m (145 d) from the mixing point.

The two gauge pressure transducers used were WIKA pressure transmitter model S-11, with a gauge pressure range of 0~6 bar, over pressure limit 35 bar, accuracy within ±0.25% of span, and time response less than 10 ms. The differential pressure transducer used was GE Sensing DRUCK PMP 4170, with pressure range -200 to +200 mbar and accuracy ±0.08 % of full scale. Both the gauge pressure transducers and the differential pressure transducer were used in our experimental runs associated with relatively small pressure drops, which includes our major tests when water is the continuous phase. Only the gauge pressure transducers were used in experimental runs associated with high pressure drop such as single oil flow tests at higher oil flow rates.

During tests, the flow upstream of the second pressure transducer was recorded using a digital HD video camera recorder (Sony HDR-CX550V) at a frame rate of 60 f/s. In the present study, an optical matching box was not installed and the videos were only used to qualitatively identify flow regimes. It is noted that a transparent box filled with water to reduce optical distortion caused by refraction is required if any quantitative information is to be extracted from the photographs.

Fluids sampling section

The sampling method was used in the present study to measure the water holdup. The fluids sampling section was located downstream the visual observation and pressure drop measurement section. It contained two ball valves (BV1, BV2) placed 1.04 m (40 d) apart (see Figure 1). The fluids can be trapped between the two valves by quickly closing the two valves together. The upstream valve, BV1, was a three way T-port ball valve which diverts the flow to a bypass line while shutting off the flow in the main flow line. A sampling port line through which the sampling fluids can flow into a volume measurement equipment was connected to the middle of the horizontal sampling section. Two air hoses connecting air supply were placed near the two ball valves to flush liquids out. The liquids were collected into a graduated cylinder (capacity: 1000 ml, precision: ±10 ml) for each experimental run.

The whole volume of fluids that would be trapped in the sampling section, $V1$, was calibrated with water ($V1$=538 ml). It is noted that the collected volume of trapped fluids includes a small section of volume in the sampling port line above the valve BV3 (see Figure 1). For water-

lubricated flow, as water is always the continuous phase, the small section in the vertical port line above the valve BV3 is occupied by water. This volume, $V2$, was calibrated with water ($V2$=28 ml) before the branches were connected together. Thus, the volume of the horizontal sampling section, $V3$, can be calculated via $V3 = V1 - V2$ ($V3$=510 ml). Denoting $V4$ as the collected water volume of two-phase liquids in an experimental run, the volume of water in the horizontal sampling section, $V5$, can be expressed as $V5 = V4 - V2$. Thus, the water holdup, H_w, can be calculated as

$$H_w = \frac{V4 - V2}{V1 - V2} \tag{18}$$

The oil holdup is obtained following

$$H_o = 1 - H_w \tag{19}$$

During the experiments, the fluids became stratified quickly with water at the bottom and oil at the top once the two-phase flow was trapped in the sampling section. By opening the valve in the sampling port line, most of the water and a large amount of oil flowed into the collection cylinder under gravitational force. Then air was used to flush the remaining liquids out. As the oil is very viscous, it was difficult to completely drain the oil out of the sampling section in moderate sampling time. When most of the oil was flushed out, the drainage of the remained thin oil film on the pipe wall becomes tedious. The sampling process was stopped when no/little water was observed in the sampling section and the oil remained was in the form of thin film. Therefore, the whole volume collected for two-phase flow was always lower than the calibrated whole volume as the volume of the collected oil was less than the in situ oil volume. However, the volume of the collected water can reasonably represent the in situ water volume of the sampling section and reasonable phase holdups can be obtained following Equations (18-19).

The uncertainty for the volume measurement using the 1000 ml graduated cylinders is about ±10 ml. Uncertainty in the collected water volume due to operation factors (e.g. the waited drainage time) can also affect the accuracy of results, while it is usually ignored or not discussed in the literature. Here as a conservative estimation, assuming an uncertainty of ±20 ml in $V4$ due to operation factors, the total uncertainty in $V4$ is estimated as ±23 ml following the uncertainty propagation law (Holman, 2011). The uncertainties in $V1$ and $V2$ are estimated as

±10 ml ignoring the uncertainties due to operation factors as they were calibrated with water (easy complete drainage) and averaged values were used from serval repeated tests. The uncertainty in the water holdup obtained through Equation (18) is estimated within ±0.05 (see a detailed uncertainty analysis in Appendix A).

3.3 Experimental procedure

A series of experimental runs were conducted following a procedure introduced as below:

(1) Introduce fluids into the pipeline. At the beginning for a series of experiments, oil was introduced into the pipeline first, then water was introduced into the pipeline at the lowest possible flow rate. The water flow rate was increased for the next test in this series. This sequence of injection was applied until the inversion from oil-continuous flow to annular-water-continuous flow was observed. Once the inversion was achieved, the opposite sequence of injection, i.e., introducing water first followed by oil injection, was applied in the experiments for the practical purpose of saving oil. As the water-lubricated flow developed at very low water flow rate in the experiments, the injection sequence of introducing water first followed by oil injection was applied for the most of the tests in this study. It was observed that for the water-lubricated flow, the injection sequence affected the time for the flow to become fully developed but showed little effect on the developed flow patterns or on the measured pressure gradients.

(2) Visual observation and online data acquisition. Data from online instrumentations were collected for a duration of 30 seconds at a sampling frequency of 250 Hz when the real-time liquid flow rates and the differential pressure displayed on the LabVIEW appeared stable. At the same time, flow behaviours at the visual observation section were recorded with the high-speed camcorder.

(3) Sample collection. Once the data acquisition in Step (2) was finished, a sample of fluids for this experimental run was collected.

(4) Repeat from Step (1) to change to another flow condition (change water flow rate at a fixed oil flow rate first to cover different water flow rates, then change oil flow rate to cover different oil flow rates).

4 Results

4.1 Flow patterns

In the present study, with increase of the superficial water velocity for a fixed superficial oil velocity, the flow pattern evolves from the category of oil-continuous flow to the category of annular-water-continuous flow. There are transitional flow structures from oil-continuous to annular-water-continuous flow which is characterised with dual continuous water and oil streams moving forward spirally or dual continuous water and oil spiral flow alternating with single oil flow; these phase configurations are named inversion. The annular-water-continuous flow can be further divided into core flow, oil plugs in water and dispersed oil lumps in water; the dispersed oil lumps differ from the oil plugs in water with characteristics of the dispersed oil phase being varied and irregular shapes. Sketches of the various phase configurations in the category of annular-water-continuous flow are illustrated in Figure 2. A more detailed description of different flow patterns can be found in Shi and Yeung (2017). Figure 3 shows the change of flow patterns and pressure gradients with increase of the input water content at a constant oil flow rate. It is demonstrated that the average pressure gradient of oil-water two-phase flow starts to drop sharply when the unstable transition pattern (i.e., inversion) develops; the pressure gradient becomes stable around a low value for the stable flow patterns of core flow and oil lumps in water. Therefore, the annular-water-continuous flow, either in the specific form of core flow, oil plugs in water or oil lumps in water, is referred to as water-lubricated flow in this paper. We emphasize annular-water-continuous here to exclude other forms of water-continuous flow such as stratified flow and swirling flow which do not lubricate the pipe as efficiently as annular-water-continuous flow hence the pressure gradient is not as low as annular-water-continuous flow. Also, it is worth emphasizing that different to the ideal water-lubricated flow, oil fouling ripples on the pipe wall always existed in the present experimental study. The height of the oil fouling layer of developed water-lubricated flow was dynamically stable in the experiments. Also, no obvious difference was observed in tests conducted with the different sequences of fluids injection as introduced in Section 3.3. This indicates that the thickness of the oil fouling layer of developed water-lubricated flow is not related to the initial

flow but linked to the dynamic balance between the shear acted on the oil fouling layer from the faster-moving fluids, the gravitational force and interfacial tensions.

Figure 4 shows a typical flow pattern map of high-viscosity oil-water flow produced from the present study. It is demonstrated that water-lubricated flow is the dominating flow category for high-viscosity oil-water flow for the investigated phase velocity range (U_{so}: 0.04-0.56 m/s, U_{sw} :0.03-1 m/s). Specifically within the category of water-lubricated flow, core flow is the dominating flow regime, followed by the dispersed oil lumps. This is in consistency with experimental observations reported by Grassi et al. (2008) and Sotgia et al. (2008). The water holdup and the pressure gradients of water-lubricated flow is the focus of the present study and will be discussed in the following sections.

4.2 Water holdup of water-lubricated flow

Figure 5 shows the relation between the measured water holdups (H_w) and the input water volume fractions (C_w) under different superficial oil velocities. The error bars show estimated uncertainty in H_w (±0.05). An interesting trend demonstrated by Figure 5 is that at lower superficial oil velocities (see Figure 5 (a) and (b)), H_w is more significantly lower than C_w, indicating that the water phase is flowing faster, and oil is accumulating. Referring to the recorded flow patterns under these flow conditions, the common feature of the flow patterns is that the oil core, continuously or discontinuously flows eccentrically in the upper part of the pipe. The higher the eccentricity of the oil core (i.e., the thinner the water layer between the top of the oil and the upper wall of the pipe), the more intense the shear between the top side of the oil core and the thin water layer. In general, the higher the oil flow rate, the less eccentric the oil phase of the water-lubricated flow, hence the lower the drag force on the oil phase. This leads to lower oil holdup (i.e. higher water holdup). This can explain that H_w is closer to C_w in Figure 5 (b) than in Figure 5 (a). When the superficial oil velocity is high, the oil core is nearly concentric at a wide range of water contents due to high oil inertia. As shown in Figure 5 (e) for U_{so}=0.54 m/s, the measured water holdup is always higher than the input water volume fraction, indicating that the oil core is flowing faster than the annular water phase. At medium superficial oil velocities as shown in Figure 5 (c) and (d), the trends of H_w with C_w are like transitions between that of low oil flow rate when the eccentricity of oil phase is high and that of high oil

flow rate when the oil core is virtually concentric. Some examples of phase configurations at different superficial oil velocities for a constant C_w are shown in Figure 6. It can be observed that the eccentricity decreases with increase in the U_{so}. CFD simulaitons of core flow conducted by Shi (2015) also demonstrate that the oil core gets more concentric for higher U_{so}. Besides the oil phase eccentricity, oil fouling film on the pipe wall also affects the water holdup. As the cross-section of the oil fouling film is minor compared to that of the oil core, the contribution of oil fouling on the oil holdup is not significant.

The relation between the measured water holdups and the input water volume fractions for two different oil viscosities is shown in Figure 7. The influence of oil viscosity on the water holdup of water-lubricated flow appears to be minor for the investigated oil viscosity range in the present study.

From the measured water holdup, the oil-water slip ratio of core flow, s , can be obtained based on the mass balance ($s = U_o/U_w$; $U_o = U_{so}/(1 - H_w)$; $U_w = U_{sw}/H_w$). It should be noted that for core flow with oil fouling ripples on the pipe wall, the obtained average oil-phase velocity is slightly lower than the average oil-core velocity due to the minor contribution of the oil fouling on the oil holdup in this study. Therefore, the obtained oil-water slip ratio should be slightly lower than the average slip ratio of oil-core to water-annulus. Figure 8 shows the oil-water slip ratio of the core flow versus the input water volume fraction. The slip ratio of 1 is marked with a dash line. The oil-water slip ratio of the core flow varies from 0.5 to 1.4 for the present experimental conditions. At the lower U_{so} of 0.11 m/s, the oil-water slip ratio is lower than 1; at the higher U_{so} of 0.54 m/s, the oil-water slip ratio is higher than 1, and at the medium U_{so} around 0.2 and 0.4 m/s, the slip ratio varies around 1. The change of the oil-water slip ratio with input water volume fraction at various U_{so} corresponds to the change of the water holdup with input water volume fraction at various U_{so} which is closely related to the degree of the oil phase eccentricity as discussed above. This can explain why the limited experimental data on the water holdup or oil-water slip ratio of core flow in the literature is inconsistent with regard to the relationship between the water holdup and the input water volume fraction. Oliemans et al. (1987) reported that the average oil-water slip ratio was higher than 1 for core flow in a horizontal pipe of 50 mm I.D. It is noted that the oil phase velocity range in the experiments of

Oliemans et al. (1987) was high, ranging between 0.5 and 2.5 m/s. Also, the oil density used in in the experiments of Oliemans et al. (1987) was close to the water density with a value around 978 kg/m^3. Therefore the oil core of the core flow in the experiments of Oliemans et al. (1987) is likely to be more concentric. Bannwart (1998) reported an average oil-water slip ratio of 1 for core flow in a horizontal pipe of 22.5 mm I.D. The oil density used in Bannwart (1998) was also close to the water density with a value around 989 kg/m^3, but the oil phase velocity was not as high as that in Oliemans et al. (1987), ranging between 0.26 and 0.63 m/s. The author described that the oil core was slightly off-centred. It is possible that most of the data points from Bannwart (1998) located in the transitional region between highly eccentric and virtually concentric core flow.

From the above discussion on the water holdup/ oil-water slip ratio of water-lubricated flow, it can be concluded that the water holdup of the water-lubricated flow is not only closely related to the input water volume fraction but also the degree of oil phase eccentricity inside the continuous water. Oil fouling on the pipe wall also affect the water holdup but this influence is not significant for stable water-lubricated flow in which the oil fouling film is minor compared to the dominating oil phase. Here the degree of the eccentricity is attributed to the dimensionless Froude number, $\mathrm{Fr} = \frac{U_{so}}{\sqrt{gD\frac{\Delta\rho}{\rho_w}}}$, which reflects the ratio of the inertia to buoyancy. The oil phase of the water-lubricated flow is more concentric when the influence of oil inertia outweighs that of buoyancy. The oil phase eccentricity of the water-lubricated flow is low for high Fr, i.e., high U_{so}, or/and low $D \cdot \Delta\rho$, and vice versa.

A reliable estimate of water holdup, H_w, is needed for the calculation of the pressure gradient of the water lubricated flow in some models. Arney et al. (1993) obtained an empirical model, $H_w = C_w[1 + 0.35(1 - C_w)]$ (Equation (4)), for the prediction of the water holdup based on their own experimental data as well as data collected from the literature. The aforementioned model predicts that the water holdup of core flow is always higher than the input water volume fraction. It agrees well with data from several different sources, mainly Arney et al. (1993), Bai et al. (1992), Charles et al. (1961), and Oliemans (1987). The oil core of the core flow in the experiments of Oliemans et al. (1987) is likely to be roughly concentric as discussed above.

Similarly, the experiments by Arney et al. (1993) is likely to be nearly concentric with a small pipe (I.D=16mm), and lower phase density difference (9-13 kg/m^3). The oil core of the core flow in the experiments of Bai et al. (1992) and Charles et al. (1961) is virtually concentric due to being vertical flow, and being horizontal equal density of oil and water phases, respectively. Besides, there was no or little oil fouling on the pipe wall in the aforementioned studies due to special attention in the experimental procedures to prevent oil fouling. Therefore, the aforementioned empirical model is obtained from experimental sources of having roughly concentric core flow without oil fouling on the pipe wall and should be applied exclusively for the prediction of core flows which satisfy the aforementioned conditions.

A correlation to estimate the water holdup of core flow in wider flow conditions would be useful. A modified correlation of that proposed by Arney et al. (1993) was introduced based on our experimental data (core flow in a 1 inch horizontal pipe). The modified correlation is expressed as

$$H_w = C_w[1 + \mathrm{c}\,(1 - C_w)]C_{\mathrm{H}} \tag{20}$$

$$C_H = e^{-0.31(\frac{1}{\mathrm{Fr}})^{1.067}\,(1-C_w)^{0.67}} \tag{21}$$

$$\frac{1}{\mathrm{Fr}} = \frac{\sqrt{gD\,\frac{(\rho_w - \rho_o)}{\rho_w}}}{U_{so}} \tag{22}$$

where c is a constant, c=0.31; C_H is a coefficient associated with the oil core concentricity and oil fouling, which is defined as a function of $\frac{1}{\mathrm{Fr}}$ and C_w. Equation (20) was proposed on the basis that the empirical correlation of Arney et al. (1993) works well for virtually concentric core flow and the form of $C_w[1 + \mathrm{c}\,(1 - C_w)]$ is adopted; this part would predict a value higher than C_w. The coefficient C_H should have a value approaching 1 when the oil core is almost concentric and a value between 0 and 1 when it is eccentric. The coefficient is correlated to $\frac{1}{\mathrm{Fr}}$, and the input oil volume fraction, $1 - C_w$ ($0 < C_w < 1$). It is noted that $\frac{1}{\mathrm{Fr}}$ is treated as a dimensionless number which is the ratio of the gravitational force to the inertial force instead of the literal reciprocal of the Froude number to include the case of $\frac{1}{\mathrm{Fr}}$=0 when $\rho_w = \rho_o$. The oil core is virtually concentric when the immiscible fluids are density-matched, having $\frac{1}{\mathrm{Fr}}$=0, hence C_H=1.

The coefficients in Equations (20-22) are obtained from the experimental data of the present study.

A comparison of the model performance is shown in Figure 9 by comparing predicted values with measured counterparts from the present study. In addition to the empirical correlations, a mechanistic model for the prediction of the water holdup of by Brauner (1998) (referring to the model introduction in Section 2 Literature review) is also evaluated. It should be noted that the mechanistic model of Brauner (1998) is derived for concentric core annular flow without oil fouling on the pipe wall. As discussed above, the correlation proposed by Arney et al. (1993) was obtained from experimental sources of having roughly concentric core flow without oil fouling. From Figure 9, it can be observed that the predictions of the water holdup from the mechanistic model of Brauner (1998) and the correlation of Arney et al. (1993) have a fair agreement with experimental counterparts when the oil flow rate is high with the oil core being roughly concentric (Figure 9 (d)); the agreement decreases with decrease in the oil flow rate (from Figure 9 (c) to Figure 9 (a)). This demonstrates that simply applying the mechanistic model of Brauner (1998) and the correlation of Arney et al. (1993) to eccentric core flow for the prediction of water holdup would not give reasonable predictions. The modified correlation to that of Arney et al. (1993) proposed in the present study shows feasibility to give reasonable predictions for both concentric and eccentric core flow. In addition, the reasonable predictions from models of Arney et al. (1993) and Brauner (1998) for roughly concentric core flow with oil fouling film in the present study as shown in Figure 9 (d) also reflect that the influence of oil fouling film of stable water-lubricated flow on the water holdup is not significant.

The calculation of the water holdup with the newly proposed correlation needs information of Fr (specifically, D, ρ_w, ρ_o, and U_{so}), apart from the input water volume fraction. Comparison of the model predictions with the whole data used by Arney et al. (1993) is not achieved due to lack of detailed information. However, the new correlation is thought to have the capacity to fit the data used by Arney et al. (1993). As the majority data used by Arney et al. (1993) is from experimental sources of having concentric or roughly concentric core flow, $\frac{1}{\mathrm{Fr}}$ would be equal to or approaching to 0 for those data sources, leading to the coefficient, C_{H}, close to 1. For concentric core flow, the newly developed correlation (see Equation (20)) can be simplified to

$$H_w = C_w[1 + \mathrm{c}\,(1 - C_w)] \tag{23}$$

where c=0.31. Equation (23) is similar to the correlation of Arney et al. (1993) (see Equation (4)); the minor difference is that the coefficient in the new correlation is slightly reduced from 0.35 to 0.31. A comparison of the model predictions with the experimental data from Charles et al. (1961), which is one of the data sources used by Arney et al. (1993), is shown in Figure 10. The oil used by Charles et al. (1961) had density as equal as that of water, thus the core annular flow observed in the experiments of Charles et al. (1961) was virtually concentric. A good agreement is shown between the predicted water holdups from the proposed correlation and the measured counterparts.

It is finally worth remarking that the modified correlation to the water holdup correlation of Arney et al. (1993) is proposed and validated to be applicable for both concentric and eccentric core flows. However, as the coefficients of the correlation are obtained from the experimental data of the present study which is limited to core flow in a 1 inch pipe, the correlation should be re-evaluated as more data become available to extend its application range.

4.3 Pressure gradient of water-lubricated flow

The coefficient of resistance, λ ($\lambda = \frac{-\mathrm{d}p/\mathrm{d}z}{(\rho_\mathrm{m}/2D)U_\mathrm{m}^2}$), versus the Reynolds number of the water-lubricated two-phase flow which is defined as $\mathrm{Re} = \frac{\rho_\mathrm{m} U_\mathrm{m} D}{\mu_\mathrm{w}}$ is shown in Figure 11. For comparison, data of water-lubricated flow in the same experimental rig using a different lube oil CYL 1000 but without the fluids sampling section (see Al-Awadi, 2011 and Shi et al., 2016) is also plotted out as well as the theoretical frictional resistance of single water flow. The Colebrook–White equation (Colebrook, 1939) is used to approximate the friction factor of single water flow in both hydraulic smooth pipes and rough pipes; ε represents the roughness height in Figure 11. The friction factors of the two groups of water-lubricated flow in the same flow rig using two different oils show similar trend. For the experimental Reynolds number range between 5000 and 35 000, the friction factor of water-lubricated transport of high-viscosity oil is about one to two orders of magnitude higher than that of single water flow. With increase of the Reynolds number hence the mixture velocity, the friction factor of the water-lubricated flow shows a quicker decrease than that of single water flow. This is related to the fact that the oil

fouling on the pipe wall reduces with increase of the mixture velocity. A higher mixture velocity can result from a higher U_{so} or a higher U_{sw}. Once water-lubricated flow is developed, the oil phase is more concentric at a higher U_{so} or higher oil inertia, resulting in less oil contact of the oil with the pipe wall. Also, a higher U_{sw} can flush away the oil fouling film on the pipe wall more effectively. The group with oil CYL 1000 has in general higher friction factors than that with oil CYL 680. Since the two groups of data were conducted in the same pipeline, it is suspected that the difference is due to different wettability of the pipe wall by the two different oils which leads to different degree of oil fouling. The wettability between the Perspex pipe and oils were not measured quantitatively in the present study, but it was observed that the oil fouling on the pipe wall was generally more serious during experiments conducted with CYL 1000. A quantitative study on the influence of wettability on the pressure gradient of water-lubricated flow is recommended for future studies.

Experimental data on the pressure gradient of water lubricated flow from the present study and experiments conducted in the authors' research group (see Al-Awadi, 2011and Alagbe, 2013) were collated here to make a big database for evaluation of models. The database consists of data using two different oils (oil CYL 680, viscosity ranges between 3300 and 7100 cP; oil CYL 1000, viscosity ranges between 3800 and 16 000 cP). It contains 128 samples of core flow, and 159 samples of water-lubricated flow (i.e., core flow and oil plugs/lumps in water). The database was used to evaluate the performance of the models for the prediction of the pressure gradient of core flow or water-lubricated flow (referring to the models introduced in Section 2 Literature review). Only the data for core flow were used for the evaluation of models of core flow, including the models of Arney et al. (1993), Brauner (1998) and Bannwart (1998), while the data for water-lubricated flow were used for evaluation of models of water-lubricated flow, including models of McKibben et al. (2000b) and McKibben et al. (2013).

The models of Arney et al. (1993) and Brauner (1998) are proposed for virtually concentric core flow and the influence of oil fouling is not accounted for in the above models. It is expected that the aforementioned models would under predict the pressure gradients of core flow in the present study as well as core flow in industrial applications. However, the quantitative discrepancy of applying the above models to core flow in practical conditions is unclear.

Comparisons between measured pressure gradients of core flow and predicted counterparts from the aforementioned models are shown in Figure 12 (a). It is demonstrated that both the models under predict the pressure gradient significantly; the relative errors range below -70%. In fact, predicted pressure gradients from the two models are close to the pressure gradients of single water flow at the corresponding mixture flow rates. The ratio of the pressure gradient of core flow to the pressure gradient of single water flow at same mixture flow rate (RTW) versus the flow Reynolds number ($\mathrm{Re} = \frac{\rho_m U_m D}{\mu_w}$) is depicted in Figure 12 (b). The measured and predicted RTW versus Re are plotted in Figure 12 (b) with y-axis labelling on the left and right, respectively. The RTW from measurement ranges between 2 and 220 while the predicted RTW from the two models ranges between 0.8 and 1.2. For the model of Arney et al. (1993), the friction factor of the two-phase flow is calculated with the traditional equation for single phase flow with a deduced Reynolds number ($\Re = \frac{\rho_m U_m D}{\mu_w}[1 + \eta^4(\mathrm{m} - 1)]$) for ideal laminar CAF. As $\eta^4(\mathrm{m} - 1)$ is small, the modified Reynolds number is close to $\frac{\rho_m U_m D}{\mu_w}$, hence the predicted pressure gradient from this model is close to that of single water flow at the mixture flow rate. For the two-fluid model of core annular flow proposed by Brauner (1998), the model calculates the pressure gradient of core annular flow momentum equations of each phase; closure laws are incorporated to get solutions. Oil fouling and oil eccentricity are not accounted for in either the basic constitution of this model or the closure laws incorporated. For high-viscosity core flow of practical flow conditions, the influence of oil fouling cannot be neglected as has been demonstrated in our experimental results. Therefore, the model of Brauner (1998) underestimates the pressure gradient when the influence of oil fouling and/or oil core eccentricity on the pressure gradient is not ignorable.

The models of Arney et al. (1993) and Brauner (1998) have been evaluated previously by the group of Poesio (see Grassi et al., 1998 and Strazza et al., 2011). Different from the large deviation shown in Figure 12, a fair agreement was demonstrated when predicted pressure gradients from both models were compared with experimental data from the above authors' experiments (pipe I.D.=21 mm, oil viscosity around 800 cP, a co-axial injection device used to aid the formation of core annular flow). It is noted that in the aforementioned experiments, the

pipe was initialised with water in high flow rate to remove oil fouling on the pipe wall if any, and the reported core flow did not have oil fouling on the pipe wall. In fact, the measured pressure gradients from the above authors' experiments were close to that of single water flow at the mixture velocity. As has been demonstrated and discussed above, the models of Arney et al. (1993) and Brauner (1998) give predictions close to the pressure gradients of single water flow at the mixture flow rates. Here we further evaluated the models of Arney et al. (1993) and Brauner (1998) with the experimental data reported in Charles et al. (1961) (see Figure 13). Core annular flow in the experiments of Charles et al. (1961) was virtually concentric due to equal densities of oil and water phases. Also, oil fouling on the pipe inner wall was not reported. As shown, both models give reasonable predictions and the two-fluid model of Brauner (1998) shows better performance. From the above discussion, it can be concluded that the models of Arney et al. (1993), and Brauner (1998) can give reasonable predictions when there is no significant oil fouling on the pipe wall. The large discrepancy shown when compared to the present experimental data is essentially due to the fact that the present experimental data is outside the range of flow conditions where the above models are suitable. The influences of oil fouling on the pipe wall on the pressure gradient of core flow in engineering conditions is not ignorable.

Bannwart (2001) proposed to use the traditional expressions of the pressure gradient of single phase flow with a modified mixture viscosity and modified friction factor coefficients to estimate the pressure gradient of core flow; modified friction factor coefficients are used to account for the oil fouling on the pipe inner wall. Figure 14 shows a comparison of predicted pressure gradients from the model of Bannwart (2001) with the present experimental data. The total flow friction factor constitutes of two coefficients, b and n, which are to be determined from experimental data (see Equation (11)). Predictions from the model with the Blasius set of b and n (b=0.316, n=0.25), b and n (b=0.066, n=0.047) obtained by the above author from experiments (μ_o=2700 cP, ρ_o=989 kg/m^3, pipe I.D.=26.7 mm; oil fouling observed), and b and n tuned to fit the present experimental data are compared with the experimental counterparts in Figure 14. The dash line represents where the predicted pressure gradient is equal to the measured counterpart. It is shown that the predicted pressure gradients from the model with the

set of *b* and *n* obtained by Bannwart (2001) are generally slightly higher than that predicted with the traditional Balsius coefficients but still much lower than the measured counterparts. Similar to the present experiments, oil fouling on the pipe wall was reported in Bannwart (2001). As the oil in the experiments of Bannwart (2001) has a higher density of 989 kg/m^3, it is suspected that the core flow in the above author's experiments was more concentric hence less contact of the oil core to the pipe wall than that in our experiments. Also, it was reported that the pipe was cleaned with water before each run in the above author's experiments, while the pipe was not cleaned with water before each run in the present experiments to resemble industrial conditions. Therefore, it is very likely that the degree of oil fouling in the above author's experiments is less significant than that in the present experiments, which can explain why the model with coefficients obtained in Bannwart (2001) underestimates the pressure gradient for the present experimental data though oil fouling is accounted for by the coefficients. The set of coefficients obtained to fit the present data has a much higher *b* which reflects an overall significant influence of oil fouling on the pressure gradient. The final expression of the pressure gradient in Bannwart (2001) is approximately proportional to U_m^{2-n} (see Equation (11)). The magnitude of 2-*n* reflects the increase rate of the pressure gradient with increase of the mixture velocity. The obtained coefficient of 2-*n* to fit the present experimental data is slightly lower than 1 with n=1.1, indicating that the pressure gradient increase rate becomes slower with increase of the mixture velocity, which can be explained by the reduced oil fouling influence on the pressure gradient with increase of the mixture velocity. The model with tuned coefficients can give reasonable predictions for most of the data points (about 85% of the compared points have relative errors within ±70%). However, as the coefficients of *b* and *n* need to be determined empirically from experiments, the applicability of this model is limited.

McKibben et al. (2000b) and McKibben et al. (2013) proposed empirical correlations from their experimental data to predict the pressure gradient of water-lubricated flow. Comparisons of predicted pressure gradients from the model of McKibben et al. (2000b) and McKibben et al. (2013) with the present experimental data are shown in Figure 15 and Figure 16, respectively. The experiments of McKibben et al. (2000a, 2000b) and McKibben et al. (2013) were conducted in steel pipeline flow loops of nominal internal pipe diameters of 50, 100 and 260 mm;

viscous lube oil, heavy crude oil and bitumen were used (viscosity ranging from 620 to 91 600 cP). It is shown that when compared with the present experimental data, the correlation proposed in McKibben et al. (2000b) gives reasonable predictions; about 93% of the compared points have relative errors within ±70% for a total data points of 159. The empirical model of McKibben et al. (2000b) has a simple form of modified Fanning friction factor which is proportional to $\mathrm{Re_w}^{-1}$ (see Equation (13)), which can be linked to that the Darcy friction friction factor (four times of the Fanning friction factor) in the model of Bannwart (2001) is proportional to $\mathrm{Re_m}^{-1.1}$ to fit our experimental data (see Equation (11) and Figure 14).

The new correlation proposed in McKibben et al. (2013) has a more complex expression of Fanning friction factor which is dependent on the mixture Froude number, superficial water and oil friction factors, and the input water volume fraction (see Equation(16)). Compared to the earlier correlation proposed by McKibben et al. (2000b) which uses a modified friction factor accounting for the overall influences of different factors, the merit of this new model lies in its constitution from which influences of water lubrication, oil fouling on the pipe inner wall (reflected in the oil phase friction factor) and oil phase eccentricity (reflected in the Froude number which is the ratio of the inertial force versus buoyancy force) are more clearly accounted for. However, the performance of this correlation is not as good as the earlier one when compared with the present experimental data. The new correlation has less underestimations while more overestimations; about 89% of the compared points have relative errors between -40% and +100%, and some predicted pressure gradients are 5 times as high as the measured values. However, less underestimation is an advantage from the perspective of safety design.

It is noted that the accuracy of different models in predicting the pressure gradient of water-lubricated high-viscosity oil-water flow is not high in general; the highest accuracy achieved for the present data base is within ±70% with the model of McKibben et al. (2000b). Oil fouling on the pipe wall has a significant influence on the pressure gradient of water-lubricated transport of high-viscosity oil. It is difficult to accurately account for the influences of oil fouling and oil core eccentricity on the pressure gradient which are associated with different parameters such as input water volume fraction, oil viscosity, Froude number and the wettability of the pipe by the oil

(pipe materials and oil properties). The influences of oil fouling and oil phase eccentricity are not considered in the models of Arney (1993) and Brauner (1998). The overall influences of the different parameters are accounted for in models of Bannwart (2001), McKibben et al. (2000b). Influences attributed from major parameters are accounted for in the models of McKibben et al. (2013). Work to further develop the model of water-lubricated high-viscosity oil-water flow is needed to improve the prediction accuracy.

5 Conclusions

In this paper, models for the prediction of the water holdup and/or the pressure gradient of core flow or water-lubricated high-viscosity oil-water flow were reviewed. An experimental campaign was conducted to measure the water holdup as well as the pressure gradients of water-lubricated high-viscosity oil two-phase flow. Evaluation of the existing models was conducted with light shed on the applicability range of different models. The major findings from this study are summarised as follows.

The water holdup (H_w) of the water-lubricated flow is not only closely related to the input water volume fraction (C_w) but also the degree of oil phase eccentricity which are attributed to the phase Froude number, $\mathrm{Fr} = \frac{U_{so}}{\sqrt{gD\frac{\Delta\rho}{\rho_w}}}$. For the prediction of the water holdup, the models of Arney et al. (1993) and Brauner (1998) can give reasonable predictions when the oil core is virtually concentric. However, as the eccentricity degree of the oil core becomes higher the models tend to over predict the water holdup. A modified correlation to the water holdup correlation of Arney et al. (1993) was proposed in the present study by introducing a coefficient which is to account for the influences of oil phase eccentricity and oil fouling. This correlation was evaluated and a fair applicability was shown. It is noted that this correlation should be re-evaluated as more data become available to extend its application range.

For the prediction of the pressure gradient, it is shown that the models of Arney et al. (1993) and Brauner (1998) can give reasonable predictions for core flow without oil fouling on the pipe wall and should be applied exclusively for the prediction of core flow without oil fouling. The empirical model of McKibben et al. (2000b) is found to be able to give reasonable pressure gradient predictions for water-lubricated transport of high-viscosity oil with relative errors within

±70% for most of the data points. The accuracy of different models in predicting the pressure gradient of water-lubricated transport of high-viscosity oil is not high in general. This is closely associated with the difficulty in accurately accounting for the influence of oil fouling on the pressure gradient. Further work to improve the models are needed in the future.

Appendix A. Uncertainty analysis

In this section we present the uncertainty analysis associated with the calculated variables in this study.

Suppose R is a function of the independent variables $R = R(x_1, x_2, \dots, x_n)$ and $w_1, w_2, \dots, w_n$ are uncertainties in the independent variables. If the uncertainties in the independent variables are all given with the same odds, the uncertainty in R, denoting as w_R, can be obtained as (Holman, 2011):

$$w_R = \sqrt{(\frac{\partial R}{\partial x_1} w_1)^2 + (\frac{\partial R}{\partial x_2} w_2)^2 + \cdots + (\frac{\partial R}{\partial x_n} w_n)^2} \tag{24}$$

The superficial water and oil velocities are obtained as $U_{sw} = \frac{Q_w}{A} = \frac{4Q_w}{\pi d^2}$, and $U_{so} = \frac{Q_o}{A} = \frac{4M_o}{\rho_o \pi d^2}$, respectively. The uncertainties in U_{sw} and U_{so} can be estimated as

$$w_{U_{sw}} = \sqrt{(\frac{\partial U_{sw}}{\partial Q_w} w_{Q_w})^2 + (\frac{\partial U_{sw}}{\partial \mathrm{d}} w_{\mathrm{d}})^2} \tag{25}$$

$$\frac{\partial U_{sw}}{\partial Q_w} = \frac{4}{\pi d^2} \tag{26}$$

$$\frac{\partial U_{sw}}{\partial \mathrm{d}} = -\frac{8Q_w}{\pi d^3} \tag{27}$$

$$w_{U_{so}} = \sqrt{(\frac{\partial U_{so}}{\partial M_o} w_{M_o})^2 + (\frac{\partial U_{so}}{\partial \rho_o} w_{\rho_o})^2 + (\frac{\partial U_{so}}{\partial \mathrm{d}} w_{\mathrm{d}})^2} \tag{28}$$

$$\frac{\partial U_{so}}{\partial M_o} = \frac{4}{\rho_o \pi d^2} \tag{29}$$

$$\frac{\partial U_{so}}{\partial \rho_o} = -\frac{4M_o}{{\rho_o}^2 \pi d^2} \tag{30}$$

$$\frac{\partial U_{so}}{\partial \mathrm{d}} = -\frac{8M_o}{\rho_o \pi d^3} \tag{31}$$

Combining Equations (25-27) and (28-31), the relative errors $\frac{w_{U_{sw}}}{U_{sw}}$ and $\frac{w_{U_{s0}}}{U_{s0}}$ are expressed as

$$\frac{w_{U_{sw}}}{U_{sw}} = \sqrt{(\frac{w_{Q_w}}{Q_w})^2 + (2\frac{w_{\mathrm{d}}}{\mathrm{d}})^2} \tag{32}$$

$$\frac{w_{U_{so}}}{U_{so}} = \sqrt{(\frac{w_{M_o}}{M_o})^2 + (\frac{w_{\rho_o}}{\rho_o})^2 + (2\frac{w_{\mathrm{d}}}{\mathrm{d}})^2} \tag{33}$$

where Q_w denotes the volumetric flow rate of water, M_o the mass flow rate of oil, ρ_o the oil density and d the pipe inner diameter. The uncertainties in Q_w, M_o, ρ_o and d are ±0.5% o.r. (of reading), ±0.1% o. r., ±0.5 kg/m^3 and ±0.02 mm in this study. Following Equation (32), the estimated relative error in U_{sw} is ±0.52%. The relative error in U_{so} varies for different oil densities (see Equation (33)). However, as the uncertainty caused by density is insignificant and the oil density difference was not high in our experiments, the estimated relative error in U_{s0} is around ±0.19%.

The input water volume fraction is obtained following $C_w = \frac{Q_w}{Q_w+Q_o} = \frac{1}{1+\frac{Q_o}{Q_w}} = \frac{1}{1+\frac{M_o}{Q_w\rho_o}}$ .The uncertainty in C_w can be estimated as:

$$w_{C_w} = \sqrt{(\frac{\partial C_w}{\partial Q_w}w_{Q_w})^2 + (\frac{\partial C_w}{\partial M_o}w_{M_o})^2 + (\frac{\partial C_w}{\partial \rho_o}w_{\rho_o})^2} \tag{34}$$

$$\frac{\partial C_w}{\partial Q_w} = \frac{M_o}{\left(1+\frac{M_o}{Q_w\rho_o}\right)^2 {Q_w}^2\rho_o} \tag{35}$$

$$\frac{\partial C_w}{\partial M_o} = -\frac{1}{\left(1+\frac{M_o}{Q_w\rho_o}\right)^2 Q_w\rho_o} \tag{36}$$

$$\frac{\partial C_w}{\partial \rho_o} = \frac{M_o}{\left(1+\frac{M_o}{Q_w\rho_o}\right)^2 Q_w{\rho_o}^2} \tag{37}$$

The uncertainties in Q_w, M_o, ρ_o are ±0.5% o.r., ±0.1% o. r., and 0.5 kg/m^3 in this study. The calculated uncertainties in C_w for our experiment study varied between 0.0002 and 0.001 (relative errors varied between 0.02% and 0.4%), with higher uncertainty at lower input water volume fraction (see Figure 17).

The water holdup is obtained following $H_w = \frac{V4-V2}{V1-V2}$ (see Section 3.2 for detail). The uncertainty in H_w is estimated as

$$w_{H_w} = \sqrt{(\frac{\partial H_w}{\partial V4} w_{V4})^2 + (\frac{\partial H_w}{\partial V2} w_{V2})^2 + (\frac{\partial H_w}{\partial V1} w_{V1})^2} \quad (38)$$

$$\frac{\partial H_w}{\partial V4} = \frac{1}{V1 - V2} \quad (39)$$

$$\frac{\partial H_w}{\partial V2} = \frac{V4 - V1}{(V1 - V2)^2} \quad (40)$$

$$\frac{\partial H_w}{\partial V1} = -\frac{V4 - V2}{(V1 - V2)^2} \quad (41)$$

where $V1$ and $V2$ are whole volume of the sampling section and volume in the vertical port line, respectively (see Section 3.2 for detail). They were constants obtained by calibrating with water. The uncertainties in $V1$ and $V2$ are estimated as ±10 ml. $V4$ are the water volume in collected samples. The uncertainty in $V4$ are estimated as ±23 ml (see Section 3.2 for detail). From Equations (38-41), it can be seen that w_{H_w} caused by uncertainty propagation from $V1$ and $V2$ is insignificant compared to that caused from $V4$. The estimated uncertainty in calculated water holdup is within ±0.05.

The pressure gradient is obtained as $-\mathrm{d}p/\mathrm{dz} = \frac{\Delta p}{\Delta z}$. The uncertainty in $-\mathrm{d}p/\mathrm{dz}$ is estimated as

$$w_{-\mathrm{d}p/\mathrm{dz}} = \sqrt{(\frac{\partial(-\mathrm{d}p/\mathrm{dz})}{\partial \Delta p} w_{\Delta p})^2 + (\frac{\partial(-\mathrm{d}p/\mathrm{dz})}{\partial \Delta z} w_{\Delta z})^2} \quad (42)$$

$$\frac{\partial(-\mathrm{d}p/\mathrm{dz})}{\partial \Delta p} = \frac{1}{\Delta z} \quad (43)$$

$$\frac{\partial(-\mathrm{d}p/\mathrm{dz})}{\partial \Delta z} = -\frac{\Delta p}{\Delta z^2} \quad (44)$$

where Δp denotes measurement from the differential pressure transducer, and Δz the distance across which the pressure difference is measured. The uncertainties in Δp is ±0.08% of full scale (-200 to +200 mbar) and the uncertainty in Δz is 1 mm. The estimated uncertainty in the pressure gradient is within ±19 Pa/m.

References

Al-Awadi, H., 2011. Multiphase characteristics of high viscosity oil. PhD thesis, Cranfield University, UK.

Alagbe, S. O., 2013. Experimental and numerical investigation of high viscosity oil-based multiphase flows. PhD thesis, Cranfield University, UK.

Arney, M. S., Bai, R., Guevara, E., Joseph, D., Liu, K., 1993. Friction factor and holdup studies for lubricated pipelining—I. Experiments and correlations. International journal of multiphase flow, 19(6), pp. 1061-1076.

Arney, M. S., Ribeiro, G. S., Guevara, E., Bai, R., Joseph, D. D., 1996. Cement-lined pipes for water lubricated transport of heavy oil. International journal of multiphase flow, 22(2), pp. 207-221.

Bai, R., Chen, K., Joseph, D., 1992. Lubricated pipelining: stability of core-annular flow. Part 5. Experiments and comparison with theory. J. Fluid Mech, 240(97), pp. 132.

Bai, R., Kelkar, K., Joseph, D. D., 1996. Direct simulation of interfacial waves in a high-viscosity-ratio and axisymmetric core–annular flow. Journal of Fluid Mechanics, 327, pp. 1-34.

Bannwart, A. C., 1998. Wavespeed and volumetric fraction in core annular flow. International journal of multiphase flow, 24(6), pp. 961-974.

Bannwart, A. C., 2001. Modeling aspects of oil–water core–annular flows. Journal of Petroleum Science and Engineering, 32(2), pp. 127-143.

Bannwart, A. C., Rodriguez, O. M., de Carvalho, C. H., Wang, I. S., Vara, R. M., 2004. Flow patterns in heavy crude oil-water flow. Journal of energy resources technology, 126(3), 184-189.

Beerens, J. C., Ooms, G., Pourquie, M. J., Westerweel, J., 2014. A comparison between numerical predictions and theoretical and experimental results for laminar core‐annular flow. AIChE Journal, 60(8), pp. 3046-3056.

Brauner, N.,1998. Liquid-liquid two-phase flow. in Hewitt, G. F., (ed.) Heat Exchanger Design Handbook.

Charles, M. E., Govier, G. t., Hodgson, G., 1961. The horizontal pipeline flow of equal density oil-water mixtures. The Canadian Journal of Chemical Engineering, 39(1), pp. 27-36.

Colebrook, C. F., 1939. Turbulent Flow in Pipes, with particular reference to the Transition Region between the Smooth and Rough Pipe Laws. Journal of the ICE, 11(4), pp. 133-156.

Grassi, B., Strazza, D., Poesio, P., 2008. Experimental validation of theoretical models in two-phase high-viscosity ratio liquid–liquid flows in horizontal and slightly inclined pipes. International journal of multiphase flow, 34(10), pp. 950-965.

Holman, J. P., 2011. Experimental methods for engineers, 8 ed., New York: McGraw-Hill.

Joseph, D. D., Bai, R., Mata, C., Sury, K., Grant, C., 1999. Self-lubricated transport of bitumen froth. Journal of Fluid Mechanics, 386, pp. 127-148.

Ko, T., Choi, H., Bai, R., Joseph, D., 2002. Finite element method simulation of turbulent wavy core–annular flows using a k-ω turbulence model method. International journal of multiphase flow, 28(7), 1205-1222.

Lee, B., Kang, M., 2016. Full 3d simulations of two-phase core–annular flow in horizontal pipe using level set method. Journal of Scientific Computing, 66(3), pp. 1025-1051.

Li, J., Renardy, Y., 2000. Numerical study of flows of two immiscible liquids at low Reynolds number. SIAM review, 42(3), 417-439

McKibben, M. J., Gillies, R. G., Shook, C. A., 2000a. A laboratory investigation of horizontal well heavy oil—water flows. The Canadian Journal of Chemical Engineering, 78(4), pp. 743-751.

McKibben, M. J., Gillies, R. G., Shook, C. A., 2000b. Predicting pressure gradients in heavy oil—water pipelines. The Canadian Journal of Chemical Engineering, 78(4), pp. 752-756.

McKibben, M. J., Sanders, R. S., Gillies, R. G., 2013. A New Method for Predicting Friction Losses and Solids Deposition during the Water-Assisted Pipeline Transport of Heavy Oils and Co-Produced Sand. in SPE Heavy Oil Conference-Canada,Alberta, Canada,11-13 June, 2013.

Oliemans, R. , Ooms, G., 1986. Core-annular flow of oil and water. Multiphase Science and Technology, 2(1-4), 427-476.

Oliemans, R., Ooms, G., Wu, H., Duijvestijn, A., 1987. Core-annular oil/water flow: the turbulent-lubricating-film model and measurements in a 5 cm pipe loop. International journal of multiphase flow, 13(1), pp. 23-31.

Ooms, G., Segal, A., Van Der Wees, A., Meerhoff, R., Oliemans, R., 1984. A theoretical model for core-annular flow of a very viscous oil core and a water annulus through a horizontal pipe. International journal of multiphase flow, 10(1), pp. 41-60.

Ooms, G., Pourquie, M., Beerens, J., 2013. On the levitation force in horizontal core-annular flow with a large viscosity ratio and small density ratio. Physics of Fluids, 25(3), pp. 032102.

Shi, J., 2015. A study on high-viscoisty oil-water two-phase flow in horizontal pipes, PhD thesis, Cranfield University, Cranfield, UK 2015, p. 195-222.

Shi, J., Yeung, H., 2017. Characterization of liquid-liquid flows in horizontal pipes. AIChE Journal, 63(3), pp. 1132-1143.

Shi, J, Al-Awadi, H., Yeung, H. An experimental investigation of high-viscosity oil-water flow in a horizontal pipe. The Canadian Journal of Chemical Engineering, submitted for publication, 2016.

Sotgia, G., Tartarini, P., Stalio, E., 2008. Experimental analysis of flow regimes and pressure drop reduction in oil–water mixtures. International journal of multiphase flow, 34(12), pp. 1161-1174.

Sridhar, S., Zhang, H.-q., Sarica, C., Pereyra, E. J., 2011. Experiments and Model Assessment on High-Viscosity Oil/Water Inclined Pipe Flows. in SPE Annual Technical Conference and Exhibition, Colorado, USA, 30 October-2 November, 2011.

Strazza, D., Demori, M., Ferrari, V., Poesio, P., 2011a. Capacitance sensor for hold-up measurement in high-viscous-oil/conductive-water core-annular flows. Flow Measurement and Instrumentation, 22(5), pp. 360-369.

Strazza, D., Grassi, B., Demori, M., Ferrari, V., Poesio, P., 2011b. Core-annular flow in horizontal and slightly inclined pipes: Existence, pressure drops, and hold-up. Chemical Engineering Science, 66(12), pp. 2853-2863.

Wang, W., Gong, J., Angeli, P., 2011. Investigation on heavy crude-water two phase flow and related flow characteristics. International journal of multiphase flow, 37(9), pp. 1156-1164.

Table Captions

Table 1. Summary of experimental studies on high-viscosity oil-water flow in horizontal pipes.

Table 2. A summary of flow models of core annular flow (CAF) or water-lubricated flow.

Table 3. Oil physical properties.

Figure Captions

Figure 1. Schematic of the experimental setup.

Figure 2. Sketches of phase configurations in the category of annular-water-continuous flow. (a, b)- Core flow; (c)- Oil plugs in water; (d)- Oil lumps in water.

Figure 3. Flow patterns at different input water volume fraction and the corresponding pressure gradients (U_{so}=0.1m/s, oil viscosity around 5600 cP).

Figure 4. Flow map of high-viscosity oil-water flow for nominal oil viscosity around 5600 cP.

Figure 5. Water holdup (H_w) versus input water volume fraction (C_w) at various U_{so} (μ_o=5600 cP). (a) U_{so}=0.04 m/s; (b) U_{so}=0.1 m/s; (c) U_{so}=0.2 m/s; (d) U_{so}=0.4 m/s; (e) U_{so}=0.54 m/s.

Figure 6. Phase configurations at different U_{so} at C_w around 0.5 (oil viscosity around 5600 cP). (a) U_{so}=0.1 m/s; (b) U_{so}=0.2 m/s; (c) U_{so}=0.4 m/s.

Figure 7. Water holdup (H_w) versus input water volume fraction (C_w) at various U_{so} for two different nominal oil viscosities.

Figure 8. Oil-water slip ratio of core flow versus input water volume fraction (C_w) at various U_{so} (μ_o=5600 cP).

Figure 9. Performance evaluation of different models for the prediction of water holdup of core flow (experimental data from the present study, oil viscosity around 3300 cP and 5600 cP). (a) U_{so}=0.04-0.06 m/s; (b) U_{so}=0.1 m/s; (c) U_{so}=0.2 m/s; (d) U_{so}=0.5 m/s.

Figure 10. Performance evaluation of the proposed correlation for the prediction of water holdup of core flow (experimental data from Charles et al., 1961).

Figure 11. Coefficient of resistance of the water-lubricated two-phase flow versus the Reynolds number and comparison with that of single water flow.

Figure 12. Comparison between measured pressure gradients (a) and RTW (b) of core flow from the present study and predicted counterparts from models of Arney et al. (1993) and Brauner (1998).

Figure 13. Comparison between measured pressure gradients of core flow from Charles et al. (1961) and predicted counterparts from models of Arney et al. (1993) and Brauner (1998).

Figure 14. Comparison between measured pressure gradients of core flow from the present study and predicted counterparts from the model of Bannwart (2001) with various sets of *b* and *n*. The bisector is also shown (the dash line).

Figure 15. Comparison between measured pressure gradients of water-lubricated flow from the present study and predicted counterparts from the model of McKibben et al. (2000b).

Figure 16. Comparison between measured pressure gradients of water-lubricated flow from the present study and predicted counterparts from the model of McKibben et al. (2013).

Figure 17. Estimated relative errors in the calculated input water volume fractions.

Table 1. Summary of experimental studies on high-viscosity oil-water flow in horizontal pipes.

Authors	Pipe I.D. (mm)	μ_o (cP)	ρ_o (kg/m^3)	Velocity range (m/s)	Reported flow patterns [a)]	Phase holdup measurement
Charles et al. (1961)	26	6.29,16.8, 65.0	998	U_{so}: 0.02-0.9; U_{sw}:0.03-1.07	CAF, I, D	Sampling method
Ooms et al. (1984)	50; 203	2300-3300; 200-2200	~970; ~955	U_{so} : ~1; U_{sw}: 0.01-0.25	CAF	-
Oliemans et al. (1987)	50	3000	978	U_{so}: 0.50-2.5; U_{sw}: 0.03-0.6	CAF	Extracted from images
Arney et al. (1993)	16	200 000-900 000; 2700	985; 989	U_{so}:0.14-1.16; U_{sw}:0.06-0.65	CAF, I	Sampling method
Bannwart (1998)	22.5	2700	989	U_{so}:0.26-0.63; U_{sw}:0.04-0.28	CAF	Extracted from images [b)]
Joseph et al. (1999)	25; 600	-	-	U_m: 0.25-2.5; U_m: 0.9-1.14	CAF [c)]	-
McKibben et al. (2000a)	53	620~960; 5300-11 200	885; 971-985	U_m:0.045; U_m:0.03~0.12	ST, I; I	-
McKibben et al. (2000b)	53; 105	5800-91 600; 7100	958-987; 958-984	U_m:0.5-1.2; U_m:0.3~0.77	CWA [d)]	-
Bannwart et al. (2004)	28	488	926	U_{so}: 0.007-2.5; U_{sw}:0.04-0.5	ST, CAF, I, D	-
Grassi et al. (2008)	21	800	886	U_{so}: 0.03-0.7; U_{sw}:0.2-2.5	ST, CAF, I, D	-
Sotgia et al. (2008)	21-40	919	889	U_{so}: 0.1-1.0; U_{sw}: 0.1-2.51	ST, CAF, I, D	-
Sridhar et al. (2011)	52	220, 1 070	884	U_{so}:0.1-1.0; U_{sw}:0.1-0.5	ST, CAF	Sampling method
Wang et al. (2011)	25	628	953	U_m:0.045; C_w: 0.1-0.7	ST, CAF, D [e)]	-
Strazza et al. (2011b)	21; 22	900	886	U_{so}: 0.03-0.7; U_{sw}:0.1-2.6	CAF, I, D	Capacitance probe
Al-Awadi(2011)	26	3800-16 000	920-938	U_{so}:0.06-0.57; U_{sw}:0.01-1.0	CAF, I	-
Alagbe (2013)	26	3 700-7100	905-920	U_{so}:0.06-0.4; U_{sw}:0.2-1.0	CAF, I	-

[a)] Different nomenclatures are used by different authors. Here only the basic flow patterns as introduced in Brauner (1998) and Shi and Yeung (2017) are listed, including ST (stratified flow), CAF (core annular flow), I (intermittent flow, including slugs/plugs/bubbles of one phase in another phase), and D (dispersed flow).

[b)] The slip ratio was obtained by the author from measured wave speeds; the phase holdup can be theoretically calculated from the slip ratio.

[c)] For bitumen froth, the CAF has oil-rich core and water-rich annulus.

[d)] The term of continuous water-assisted (CWA) flow is used by the authors to describe the flow. Specific flow regimes of CAF and I are possible phase configurations.

[e)] For emulsion, the ST and CAF have oil-rich phase and water-rich phase.

Table 2. A summary of flow models of core annular flow (CAF) or water-lubricated flow [a)]

Author	Water holdup (H_w)	Friction coefficient (λ or f)	Notes and remarks
Arney et al. (1993)	Empirical: $H_w = C_w[1 + 0.35(1 - C_w)]$	Laminar-laminar perfect CAF (theoretical): $\lambda = \frac{64}{\Re}$; Laminar-turbulent CAF (empirical): $\lambda = \frac{0.316}{\Re^{0.25}}$ ($\Re = \frac{\rho_m U_m D}{\mu_w}[1 + \eta^4(\mathrm{m} - 1)]$, $\eta = \sqrt{1 - H_w}$, $m = \frac{\mu_w}{\mu_o}$)	1. The empirical correlations for water holdup are obtained from several sources of experimental data; the application range is not clearly specified. 2. Oil fouling is not accounted for.
Brauner (1998)	Solved from two-fluid model [b)]	Solved from two-fluid model	1. It is proposed for concentric CAF. 2. Empirical closures for the calculation of interfacial and wall shear are used to solve the two-fluid model. 3. Oil fouling is not accounted for.
Bannwart (2001)	Theoretical: $1 - \frac{1}{1+s\frac{U_{sw}}{U_{so}}}$	Laminar-laminar CAF(empirical): $\lambda = 64/\left(\frac{\rho_m U_m D}{\mu_m}\right)$; ($\frac{1}{\mu_m} = \frac{1-{H_o}^2}{\mu_w}$, $H_o = \frac{1}{1+s\frac{U_{sw}}{U_{so}}}$) Laminar-turbulent CAF (empirical): $\lambda = b\left(\frac{\rho_m U_m D}{\mu_m}\right)^{-n}$ ($\frac{1}{\mu_m} = \frac{1-H_o}{\mu_w}$)	1. The slip ratio of the two fluids, $s_{i,o}$, is usually unknown; $s_{i,o}$=1 is recommended by the author when it is unknown. 2. Oil fouling is accounted for by b and n. 3. The parameters, b and n, are to be determined from experimental data, thus the applicability of this empirical model is limited.
McKibben et al. (2000b)	-	Empirical correlation for water-lubricated flow with oil fouling: $f_m = \frac{1410}{\mathrm{Re_w}}$ ($\mathrm{Re_w} = \frac{D U_m \rho_w}{\mu_w}$)	1. For water-lubricated flow with oil fouling 2. The correlation is determined from experimental data with a wide coverage of oils (viscosity between 620 and 91 600 cP) and nominal pipe diameters (50, 100 and 260 mm).
McKibben et al. (2013)	-	Empirical correlation for water-lubricated flow with oil fouling: $f_m = 15{\mathrm{Fr}_m}^{-0.5} {f_w}^{1.3} {f_o}^{0.32} {C_w}^{-1.2}$	1. Besides the above two points noted for McKibben et al. (2000b), the constitution of the new empirical model reflects influences of different parameters.

[a)] The meaning of different symbols are introduced in the text of the article.
[b)] The two-fluid model are introduced in the text of the article.

Table 3. Oil physical properties.

Oil temperature (^{o}C)	Oil viscosity (cP)	Oil density (kg/m^{3})
12	5600	910
21	3300	905

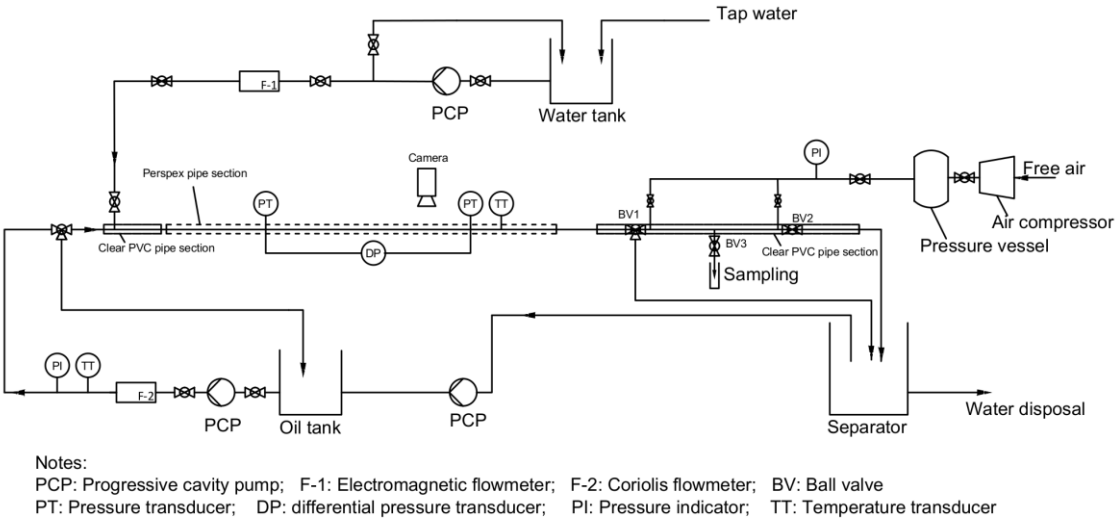

Figure 1. Schematic of the experimental setup.

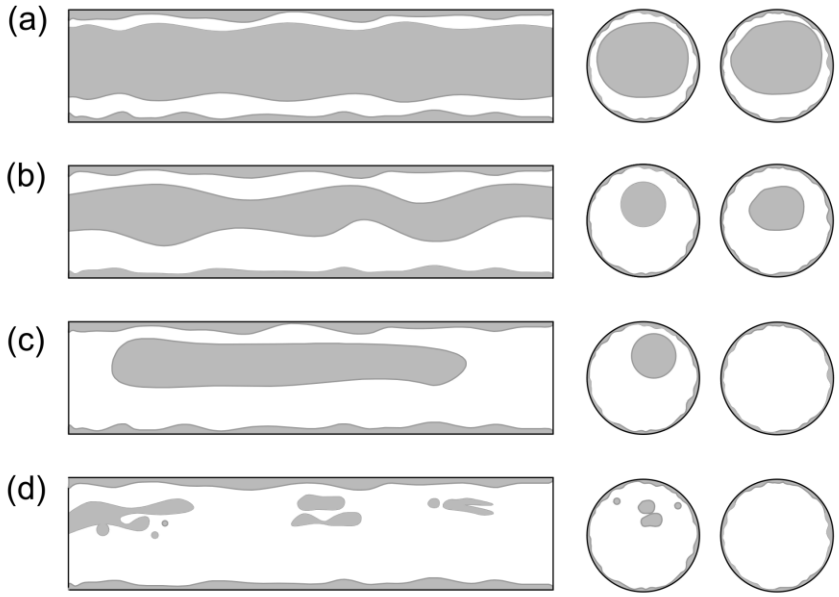

Figure 2. Sketches of phase configurations in the category of annular-water-continuous flow. (a, b)- Core flow; (c)- Oil plugs in water; (d)- Oil lumps in water.

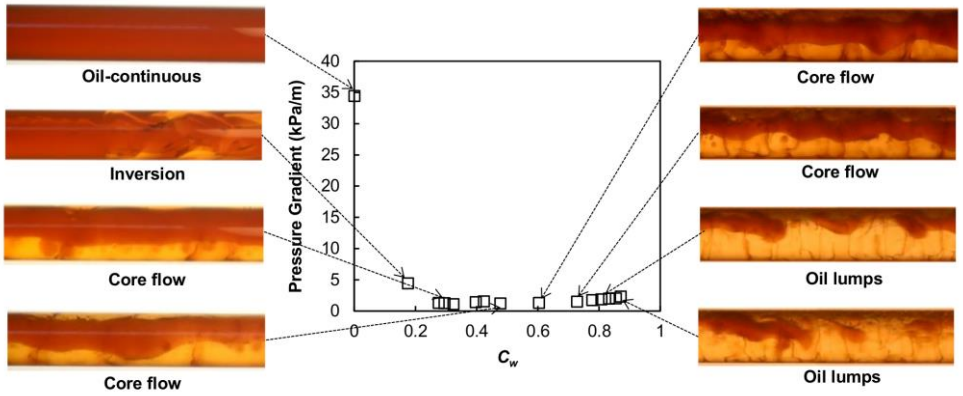

Figure 3. Flow patterns at different input water volume fraction and the corresponding pressure gradients (U_{SO}=0.1m/s, oil viscosity around 5600 cP).

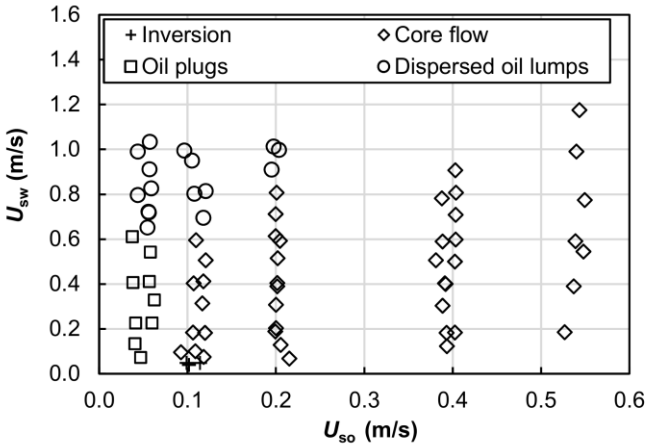

Figure 4. Flow map of high-viscosity oil-water flow for nominal oil viscosity around 5600 cP.

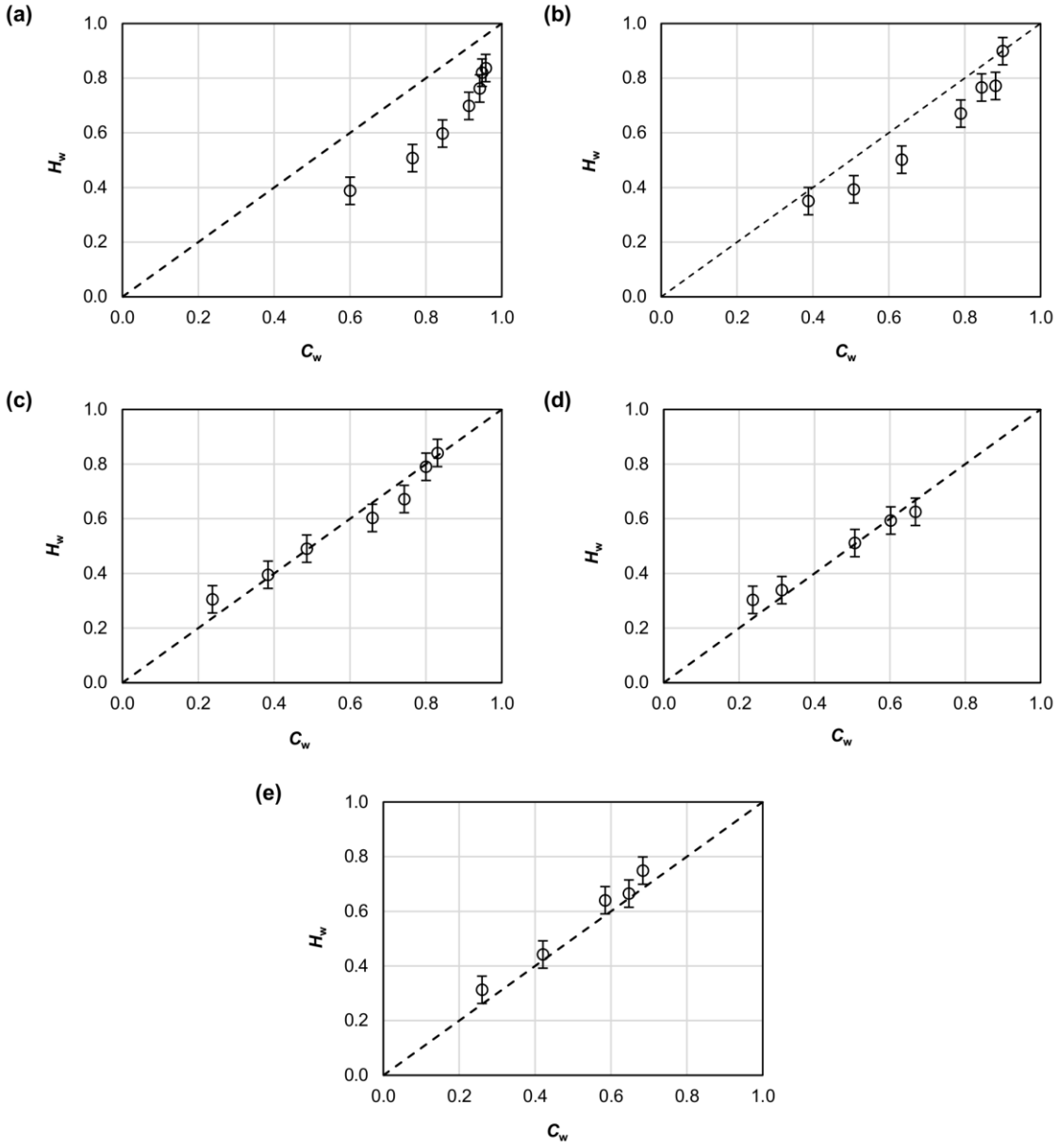

Figure 5. Water holdup (H_w) versus input water volume fraction (C_w) at various U_{so} (oil viscosity around 5600 cP). (a) U_{so}=0.04 m/s; (b) U_{so}=0.1 m/s; (c) U_{so}=0.2 m/s; (d) U_{so}=0.4 m/s; (e) U_{so}=0.54 m/s.

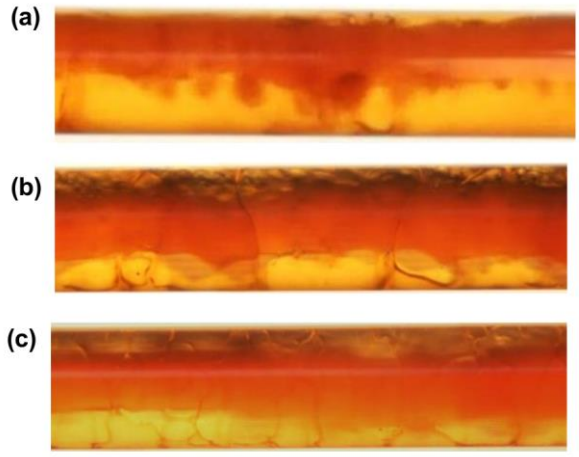

Figure 6. Phase configurations at different U_{so} at C_w around 0.5 (oil viscosity around 5600 cP). (a) U_{so}=0.1 m/s; (b) U_{so}=0.2 m/s; (c) U_{so}=0.4 m/s.

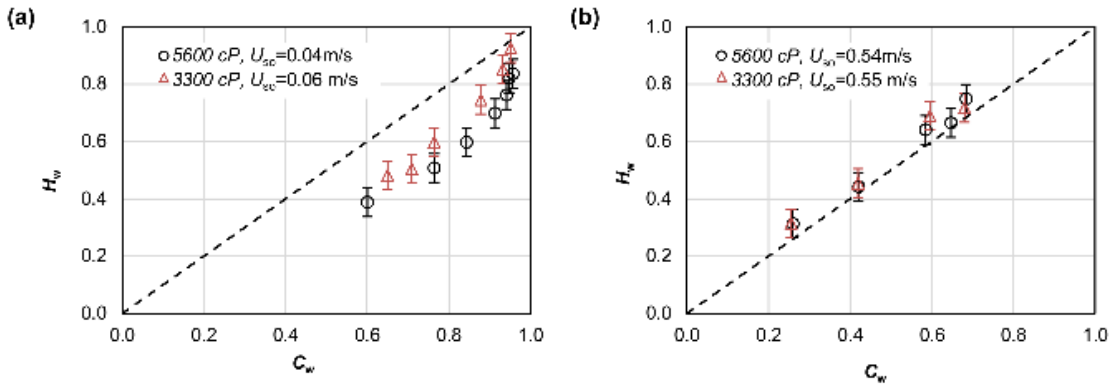

Figure 7. Water holdup (H_w) versus input water volume fraction (C_w) at various U_{so} for two different nominal oil viscosities.

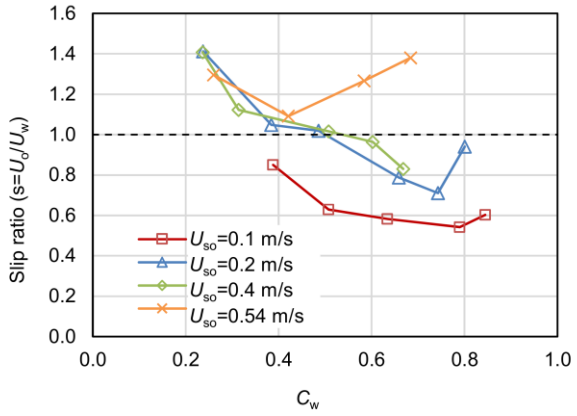

Figure 8. Oil-water slip ratio of core flow versus input water volume fraction (C_w) at various U_{so} (μ_o=5600 cP)..

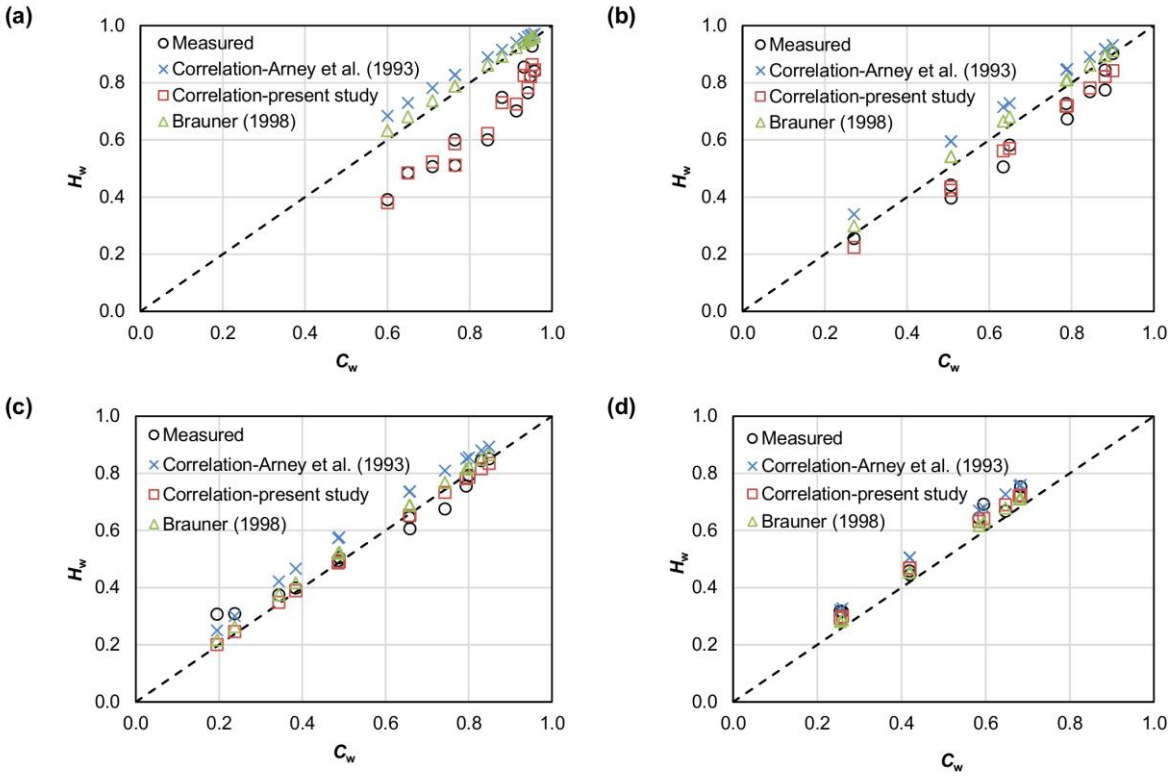

Figure 9. Performance evaluation of different models for the prediction of water holdup of core flow (experimental data from the present study, μ_o=3300 cP and 5600 cP). (a) U_{so}=0.04-0.06 m/s; (b) U_{so}=0.1 m/s; (c) U_{so}=0.2 m/s; (d) U_{so}=0.5 m/s.

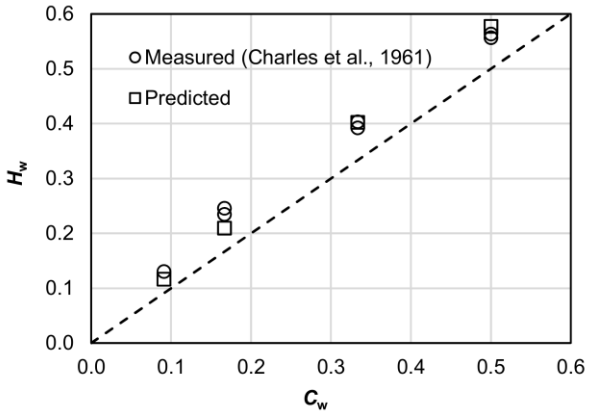

Figure 10. Performance evaluation of the proposed correlation for the prediction of water holdup of core flow (experimental data from Charles et al., 1961, μ_o=16.8 cP).

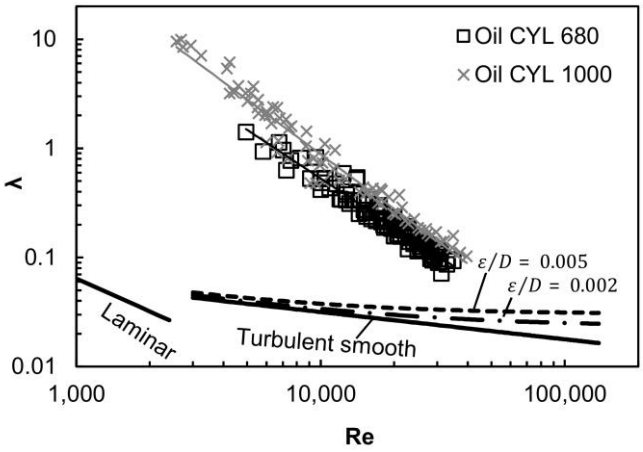

Figure 11. Coefficient of resistance of the water-lubricated two-phase flow versus the Reynolds number and comparison with that of single water flow.

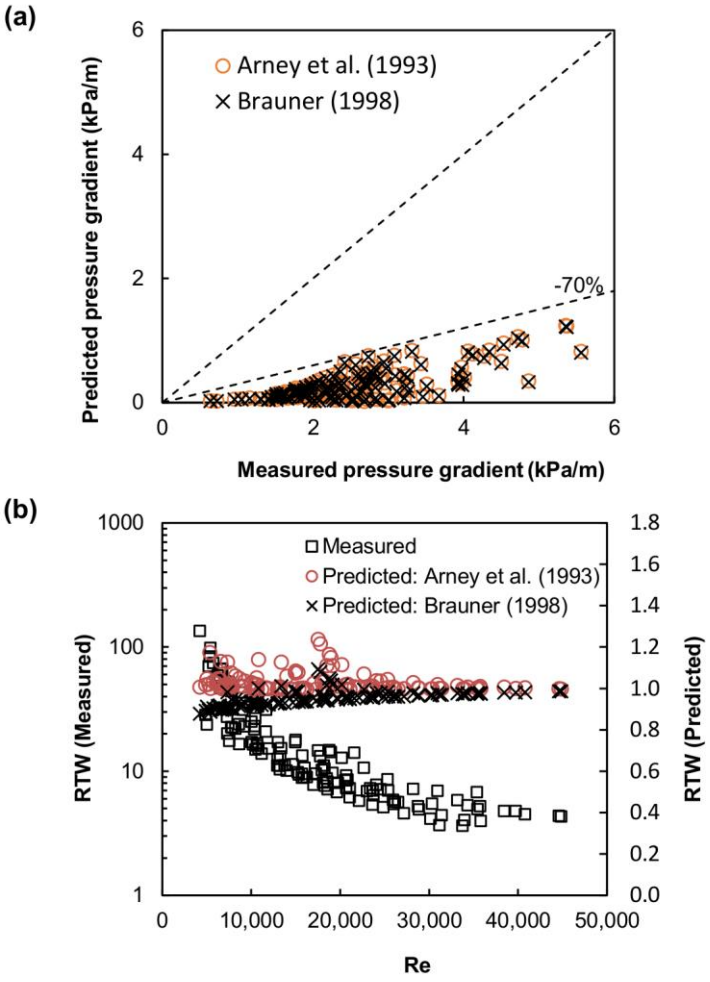

Figure 12. Comparison between measured pressure gradients (a) and RTW (b) of core flow from the present study and predicted counterparts from models of Arney et al. (1993) and Brauner (1998).

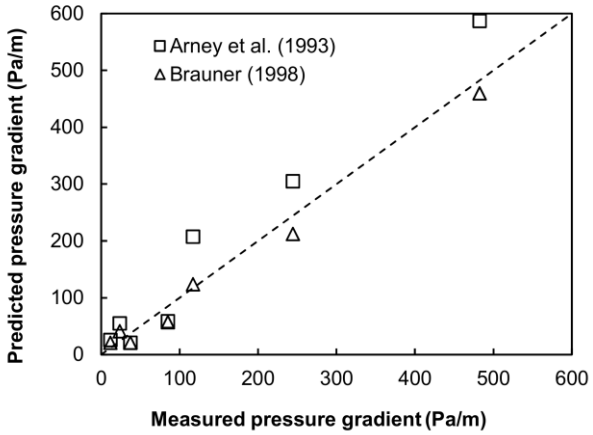

Figure 13. Comparison between measured pressure gradients of core flow from Charles et al. (1961) and predicted counterparts from models of Arney et al. (1993) and Brauner (1998).

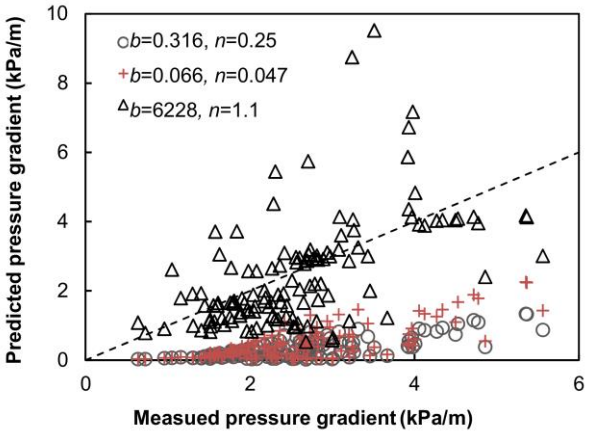

Figure 14. Comparison between measured pressure gradients of core flow from the present study and predicted counterparts from the model of Bannwart (2001) with various sets of *b* and *n*. The bisector is also shown (the dash line).

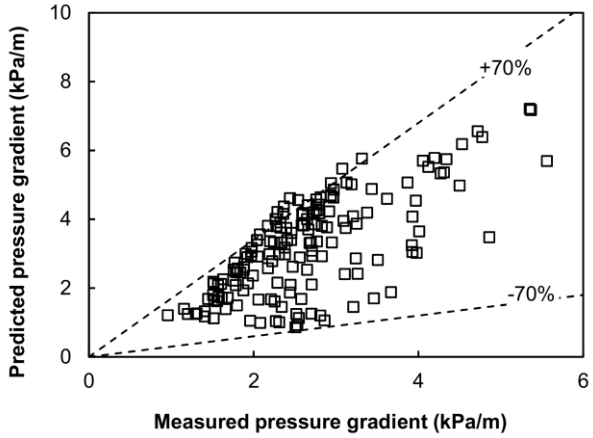

Figure 15. Comparison between measured pressure gradients of water-lubricated flow from the present study and predicted counterparts from the model of McKibben et al. (2000b).

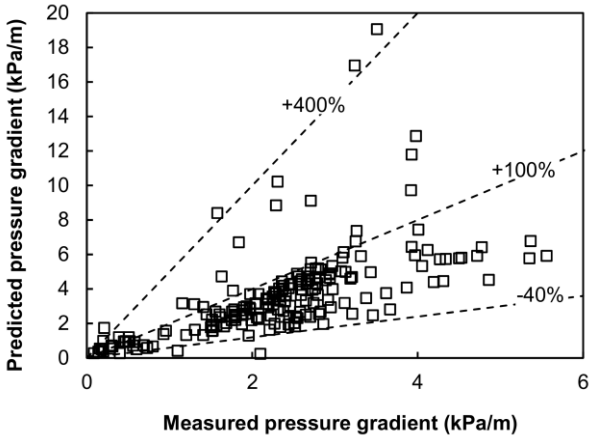

Figure 16. Comparison between measured pressure gradients of water-lubricated flow from the present study and predicted counterparts from the model of McKibben et al. (2013).

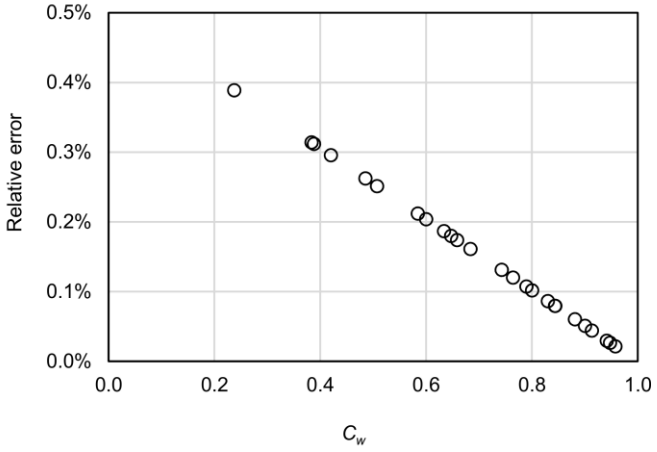

Figure 17. Estimated relative errors in the calculated input water volume fractions.